Functional and regulatory mechanisms of microtubule-associated proteins involved in cancer progression

By

Christopher R. Arnette

Dissertation

Submitted to the Faculty of the

Graduate School of Vanderbilt University

In partial fulfillment of the requirements

for the degree of

DOCTOR OF PHILOSOPHY

in

Cell and Developmental Biology

May, 2014

Nashville, Tennessee

Approved:

Susan R. Wente, Ph.D.

Alissa Weaver, M.D.,Ph.D.

Ela Knapik, M.D.

Stephen R. Hann, Ph.D.

Irina Kaverina, Ph.D.

To my loving and supportive parents, William and Rhonda, who have provided me with guidance and nurtured all of my many passions throughout my life

and

To my brothers, William and Rafael, who have loved and supported me in all that I have done

ACKNOWLEDGEMENTS

My time here at Vanderbilt has been a rollercoaster of ups and downs, but I would not trade this time for the world. In retrospect, I would say that the majority of the time here at Vanderbilt has been more ups than downs. I have grown tremendously while here, both in my knowledge of science and the scientific process, as well as personally. It goes without saying that I would never have become the scientist that I am today without the guidance, love, and support of my mentor, Irina Kaverina (Anissa). Since the day I walked into her office, she has taught me to continually strive for excellence, not only in science, but in all aspects of life. She has also taught me to think outside of the box and to not be afraid to challenge the thoughts of others. One of the most important lessons she has taught me is to be confident and unafraid to speak up. For this, I am eternally grateful. I would also like to thank my committee members for all of their suggestions and continually pushing me to become a better scientist and person: Susan Wente, Alissa Weaver, Ela Knapik, and Stephen Hann. A special thanks to Susan Wente and the Department of Cell and Developmental Biology for fostering a supporting and excellent educational environment during my time here. Moreover, the work presented in this thesis was produced with the help of funding from NIH NIGMS grant R01-GM078373-01 to I.K. and American Heart Association Grant-in-Aid 13GRNT16980096 to I.K., as well as NIH Integrated Biological Systems Training in Oncology (IBSTO) training grant 5T32CA119925-03 to C.A. and American Heart Association Predoctoral Fellowship 12PRE12040218 to C.A.

I am extremely fortunate to have had the chance to work with some excellent colleagues within as well as outside of the Kaverina Lab. To Xioadong Zhu (Sylenna), thank you for your friendship and all of your time and patience in mentoring me on scientific and non-scientific subjects. I also appreciate all the encouraging conversations and laughter that we shared which helped to make each day a little better. To Ashley Grimaldi (Tameka), I cannot imagine what life would be like without you in the Kaverina Lab. You're a pintsized fireball, who is full of knowledge and joy. I want to thank you for your friendship and all the times we've shared with one another, laughing and attending seminars/conferences, playing with Kolby and many more. To Dmitry and Maria, thank you for all the interesting times in lab and for expanding my knowledge of Russian language and culture.

Outside of the lab, I would like to give special thanks to one of my best friends, Jamille Robinson. We met on the very first day of grad school and there has never been a dull moment since. The crazy stories, late nights studying and more have made for a great distraction from grad school and provided much needed laughter and joy. Shenika Poindexter, thank you for being a sounding board and listening to me complain about experiments, as well as the heartfelt laughs and memories. Starrissa Winters, thank you for your fun-loving personality and keeping me entertained. Jeanne Jodoin, thanks for teaching me so many things and being such a great friend. I truly appreciate it. To everyone not mentioned, I want to thank you for being there for me in some way, allowing me to give you alternate names, providing me with feedback and advice, or simply inquiring about my well-being. It was all deeply appreciated and for you all, I am truly grateful to have met you.

Finally, I would like to thank my parents, William and Rhonda, as well as my brothers, William and Rafael, for all of their unyielding love and support. You all have always been in my corner and supported every decision I have ever made. You all believed in me, even when I did not believe in myself. I am very proud to be your son and brother, and I dedicate this work and effort to you all.

TABLE OF CONTENTS

Page

LIST OF FIGURES

CHAPTER I

INTRODUCTION

Microtubule Network

The cell is a fundamental unit of life, and the building block of every living thing. The importance of the cell can be witnessed in every essential life process from development to death; however, this small feat of nature would not be possible were it not for the coordinated efforts of a variety of intracellular organelles and structures that help provide regulation of the cell. One of the key components of this regulation is the cytoskeleton. The eukaryotic cytoskeleton can be divided into three main components: actin, intermediate filaments, and microtubules (MTs). The focus of this section will be on MTs and their contribution to cellular function and architecture.

MTs are hollow, cylindrical structures composed of globular α/β-tubulin heterodimers that are capable of organizing into a 13-member protofilament with an overall diameter of 25nm. MT nucleation originates at the microtubule-organizing center (MTOC), where γ-tubulin associates with other proteins to form the γ-tubulin ring complex (γ-TURC) on which α/β-tubulin heterodimers polymerize. The γ-TURC also serves as a stable platform on the minus end of polymerizing MTs. The α/β-tubulin heterodimers impart an intrinsic polarity to the protofilaments by their head-to-tail assembly. Consequently, this polarity can help define the two distinct ends of MTs: a fast-growing plus-end and a slow growing minus-end. MTs emanating from MTOCs play

specific roles in a variety of cellular events, which range from directional molecular transport, ciliary or flagellar motility, and chromosome segregation, to cytokinesis. The MT network also serves as an internal “highway system” in order to efficiently deliver cargos and organelles to distinct locations (Hirschberg *et al.*, 1998; Musch, 2004). This movement along the MTs relies on molecular motors, which carry cargo along the MT (Sheetz, 1996; Hirokawa, 1998) and generate the force necessary to transport organelles(Hall *et al.*, 1993). There are two classes of motors known to traffic along MTs: kinesins and dynein. While kinesins typically provide plus-end directed movement (Vale *et al.*, 1985; Hall and Hedgecock, 1991; Cole *et al.*, 1993), dynein provides minus-end directed movement (Schnapp and Reese, 1989; Schroer *et al.*, 1989). Specifically, kinesin-dependent transport is essential for post-Golgi cargos to be transported to the cell periphery, while dynein-dependent transport is require for retrograde transport from cell periphery to cell center (Schnapp and Reese, 1989), ER-to-Golgi transport and proper Golgi organization (Burkhardt *et al.*, 1997; Roghi and Allan, 1999). Perturbations to the MT network, such as through treatment with MT depolymerizing agent, nocodazole, leads to disorganized intracellular transport (Hirschberg *et al.*, 1998). Therefore, it is crucial that an intact MT network be maintained for efficient delivery of intercellular signals that regulate the process of cell motility.

The ability of MTs to function in all of these processes relies on their ability to assume higher-order architecture in different subcellular compartments; however, just as these structures must be assembled, they must also be disassembled. This polymerization (assembly) and depolymerization (disassembly) cycle relies on the

hydrolysis of GTP to GDP (Weisenberg *et al.*, 1976; Margolis, 1981; Carlier *et al.*, 1997), and potentially other factors. Both alpha and beta tubulin can bind GTP, but only hydrolysis of GTP on beta tubulin is thought to affect the polymerization or depolymerization state of MTs (Weisenberg *et al.*, 1976). Hydrolysis of GTP on beta tubulin weakens monomer interaction with surrounding monomers, favoring a state of MT depolymerization and influencing the dynamic state of MTs (Arnal *et al.*, 2000). As the rate of polymerization and the rate of GTP hydrolysis differ, this creates a GTP-tubulin cap at the growing MT plus-end; however loss of this cap induces rapid depolymerization (Mitchison and Kirschner, 1984). It must be noted that, once MTs begin the process of polymerization, their growth can be regulated by a unique property known as dynamic instability. This property is characterized by periods of MT growth in the presence of a GTP tubulin cap and MT depolymerization when hydrolysis of GTP tubulin to GDP tubulin reaches the + tip of the MT (Kirschner and Mitchison, 1986). These distinct phases in MT dynamics are classified into three categories. The switch from MT growth to MT depolymerization is termed catastrophe. The switch from MT shrinking to MT growth is termed rescue. Lastly, the period of time that results between periods of growth and shrinking is termed pausing.

The complete disassembly of MTs without appropriate cellular cues would lead to cellular deregulation. Dynamic instability leads to continual turnover of the MT network and is critical for the necessary remodeling of the MT network in response to the constantly changing cellular environment (Gundersen *et al.*, 2004; Mattie *et al.*, 2010). This is an important feature, as the MT network plays crucial roles in cellular

organization and dynamics in both mitotic and interphase cells. In mitotic cells, the MT network organizes into astral and kinetochore fiber subsets that are crucial for proper chromosome alignment and segregation during cell division. In motile interphase cells, the MT network organizes an asymmetric array that modulates delivery of cargos to distinct cellular domains (Sheetz, 1996; Small and Kaverina, 2003; Noritake *et al.*, 2005; Watanabe *et al.*, 2005). This ability of the MT network to assume an asymmetrical arrangement aids in the polarized remodeling of the actin cytoskeleton (Krendel *et al.*, 2002; Rodriguez *et al.*, 2003; Bretscher, 2005; Siegrist and Doe, 2007), as well as facilitating efficient focal adhesion turnover at the leading and trailing edge of migrating cells (Chabin-Brion *et al.*, 2001; Ezratty *et al.*, 2005). Therefore, the ability of the MT network to be remodeled must be precisely regulated to prevent abrupt changes in cellular architecture or disruption in the spatiotemporal distribution of organelles and signaling molecules.

Microtubule Associated Proteins (MAPs)

As the MT network comprises a large part of the eukaryotic cytoskeleton, subsets of proteins that are capable of interacting with tubulin have arisen. There are two major classes of microtubule-associated proteins (MAPs): structural MAPs and motor proteins. The term “structural MAPs” refers to the ability of these proteins to bind, stabilize, and promote the assembly of MTs. Prototypical members of this class of MAPs include: MAP1a, MAP1b, MAP4, Tau, and others, while motor proteins are represented by the two major classes, dynein and kinesins (Mandelkow and Mandelkow, 1995; Marx *et al.*, 2005).

Structural MAPs typically have repeating domains, which allows for the interaction of the MAP with multiple tubulin dimers. This ability to interact with more than one dimer is thought to aid in the ability of the MAPs to influence polymerization rates of MTs. This interaction not only stabilizes the tubulin dimers, but also imparts stability by crosslinking several subunits at once. The binding and unbinding of structural MAPs, however, must be tightly regulated to coordinate with multiple cellular processes. Structural MAPs are regulated by both kinases and phosphatases (Cassimeris and Spittle, 2001). In mitosis, for example, MAPs must be phosphorylated by kinases, such that they detach from the MT lattice; however, at the end of mitosis, these proteins must be dephosphorylated so that they regain the ability to interact with tubulin. Additionally, structural MAPs assist in motor transport by creating space around MTs (Chen *et al.*, 1992). Therefore, the ability of MTs to interact with associating proteins is necessary to regulate MT dynamics, as well as trafficking along the MT.

MT motor proteins are typically comprised of three domains: a head, a stalk, and a tail. It must be noted that the number of heads associated with a particular motor varies. Typically, the head region contains an ATP-binding site that allows for movement, in addition to the nucleotide-dependent MT-binding site. The stalk region of motor proteins is mainly responsible for the flexibility and ability of the protein to homo-dimerize. The tail region is responsible for interacting with specific cargo proteins (Stewart *et al.*, 1991; Schnapp, 2003).

In addition to associating with the MT network and influencing the dynamics of MTs, MAPs can also have various other functions. For instance, RAS-Association

Domain Family 1A (RASSF1A) can also function as a tumor suppressor and scaffold for apoptotic machinery. Additionally, MT-associated GEF-H1 can influence actin polymerization by interacting with Rho GTPases. MT association serves not only as a way to regulate these proteins, but also provides a scaffold on which they can exert their function.

RASSF1A

Ras-association domain family member 1A (RASSF1A) is a MAP and tumor suppressor protein that was identified to associate with MTs via a yeast-2-hybrid screen. The interaction of RASSF1A with MTs is one of the mechanism by which RASSF1A is thought to exert its tumor suppressor function. Localization of RASSF1A with the MT network is thought to occur through some yet identified domain; however, RASSF1A has been shown to bind tubulin in interphase and mitosis (Liu *et al.*, 2003; Rong *et al.*, 2004), as well as, MAP1b, C19ORF5, and MAP4 (Liu, 2002; Dallol *et al.*, 2004; Song *et al.*, 2005). When bound to MTs, RASSF1A can promote MT stabilization (Liu *et al.*, 2003; Dallol *et al.*, 2004; Song *et al.*, 2004; Vos *et al.*, 2004), and potentially mediate MT polymerization by acting as a scaffold with interacting partners that promote tubulin assembly. Loss of RASSF1A either through phosphorylation or other methods has detrimental effects on MT stability as well as cell-cycle progression (Dallol *et al.*, 2004). Thus, RASSF1A expression must be tightly regulated to maintain a functional MT network capable of responding to changes in cellular cues.

As mentioned above, RASSF1A is also a tumor suppressor protein that belongs to a family of RASSF proteins, of which there are eight total members, RAASF1-8. This family of proteins is so named due to the fact that they all contain Ras-association (RA) domains. However, the functionality of this domain among the different family members is quite varied, thus, its role in mediating biological effects remains unclear. The RASSF1 gene is located on chromosome 3p21.3 and contains eight exons. Through alternative splicing and differential promoter start sites, seven different transcriptional products can be made, RASSF1A-G (Dammann *et al.*, 2000; Lerman and Minna, 2000; Burbee *et al.*, 2001). The major splice variants from this region are RASSF1A and RASSF1C, both of which are ubiquitously expressed in normal tissues. Structurally, these two variants contain very similar domains. Both contain a C-terminal RalDDS/AF6 Ras-association domain (RA) necessary for mediating interactions with Ras and other small GTPases(Ponting and Benjamin, 1996; Yamamoto *et al.*, 1999) and a *Sav/RASSF/Hpo* (SARAH) domain that mediates protein-protein interactions important for cell-cycle exit and apoptosis (Scheel and Hofmann, 2003). Additionally, both proteins also contain an ataxia telagectasia mutant (ATM) domain, which may allow RASSF1A and RASSF1C to be a substrate for ATM (Kim *et al.*, 1999). However, RASSF1A also contains an additional N-terminal diaglycerol/phorbol ester-binding (DAG) domain (or protein kinase C conserved region C1), which contains a zinc finger (Newton, 1995). Though structurally very similar, the activities and regulation of RASSF1A and RASSF1C during disease are quite different, frequently resulting in loss of RASSF1A, while retaining RASSF1C expression.

Silencing of tumor suppressor genes by epigenetic modification is a fundamental inactivation mechanism of cancer-related genes in the pathogenesis of human cancer (Jones and Baylin, 2002). Particularly, promoter hypermethylation plays an essential role in loss of function of tumor suppressor genes (Herman and Baylin, 2003). Aberrant methylation of the RASSF1A promoter is found in over 40 types of sporadic human cancers (Burbee *et al.*, 2001; Pfeifer and Dammann, 2005). Loss of RASSF1A expression is associated with increased spontaneous tumor formation (Tommasi *et al.*, 2005; van der Weyden *et al.*, 2005): Likewise, ectopic expression in RASSF1A-null cancer cells lead to reduced anchorage independent growth, suppressed tumor cell growth, reduced invasiveness, and reduced tumorigenicity in vivo and in vitro (Dammann *et al.*, 2000; Burbee *et al.*, 2001; Dreijerink *et al.*, 2001; Kuzmin *et al.*, 2002; Chow *et al.*, 2004; Hesson *et al.*, 2004). Therefore, RASSF1A functions as a tumor suppressor, via regulation of the MT dynamics, that is required for proper cellular maintenance, particularly in the formation of cellular architecture and cell migration; however, many questions related to the biological function of RASSF1A, specifically in interphase, continue to remain unanswered.

GEF-H1 and other Rho GEFs

The cytoskeleton, particularly MTs, provides a network on which many signaling and regulatory molecules localize; therefore, alterations to the cytoskeleton can cause changes in intracellular signaling events (Williamson *et al.*, 1996; Jesuthasan and Stahle, 1997; Rowning *et al.*, 1997). Localization of these and other proteins are capable of interacting with the MT network to facilitate a variety processes. GEF-H1 and

p190RhoGEF are both MAPs that are regulated by MTs. MTs regulate the activity of GEF-H1 and p190RhoGEF, through binding to the MT lattice. This binding effectively inactivates GEF-H1(Birkenfeld *et al.*, 2008; Heck *et al.*, 2012) and p190RhoGEF (van Horck *et al.*, 2001), which prevents them from interacting with their respective Rho family members. MT depolymerization can release GEF-H1 and p190RhoGEF into the cytoplasm and allow them to interact with RhoA, facilitating actin polymerization. Therefore, Rho GEFs must be tightly regulated to prevent aberrant interaction with downstream targets. Deregulation of Rho GEF activity can lead to disease progression, particularly cancer. It has been shown that several oncogenes isolated by the NIH-3T3 transformation assay are activated forms of Rho-GTPase (Cerione and Zheng, 1996). For example, several truncation mutations of GEF-H1 have been identified that abrogate MT binding, causing constitutive activation of GEF-H1 (Krendel *et al.*, 2002), which can induce cellular transformation through promoting irregular RhoA cycling (Sahai and Marshall, 2002). Overall, this indicates that activation of GEF-H1 by eliminating MT-binding sequences can cause oncogenic transformation, thus their activity must be tightly controlled. Thus, the ability of MTs to regulate and activate these specific Rho GTPase family members through the action of MT-associated GEFs is quite important. Therefore, feedback mechanisms must exist to finely tune the activity of their effects on one another.

Microtubules and Rho GTPases

There has been a myriad of evidence that supports the idea that MTs are capable of regulating the Rho family of GTPases. Disruption of MTs leads to increased

vasoconstriction and agonist-induced contraction (Leite and Webb, 1998; Zhang *et al.*, 2001; Brum Cde *et al.*, 2005). It is well established that the Rho/Rho kinase pathway is a mechanism by which contraction can occur in VSMCs (Fukata *et al.*, 2001; Kawano *et al.*, 2002; Katoh *et al.*, 2011). Thus, the assembly state of MTs can affect Rho activation. The mechanism of this activation of the Rho kinase pathway is thought to occur via activation of specific Rho family members. Depolymerization of MTs activates RhoA (Liu *et al.*, 1998; Chang *et al.*, 2008; Takesono *et al.*, 2010), which re-polymerization can activate Rac1 (Waterman-Storer *et al.*, 1999; Siegrist and Doe, 2007).

Not only do MTs regulate Rho family members, but there is also evidence that Rho family members can influence MTs. Stabilization and MT rearrangement within the cell have both been shown to be a result of RhoA activation. Other Rho family members, such as Cdc42 and Rac1, can influence MT dynamics. This influence is exerted through the Pak1-mediated phosphorylation of stathmin, which is thought to promote MT growth; thus, a positive feedback loop is created whereby MTs at the leading edge activate Rac1. This Rac1, in turn, can inactivate stathmin and propagate MT growth and actin polymerization (Daub *et al.*, 2001; Wittmann *et al.*, 2003). This interplay between Rho-family members and MTs helps to create an asymmetrical MT network, which can facilitate polarization and directional cell migration; however, not only can RhoGTPases regulate MTs, but they are also capable of regulating the actin cytoskeleton, thereby impacting actin-dependent processes.

Actin regulation by Rho GTPases

Rho GTPases can also regulate the actin cytoskeleton by a well-characterized mechanism that supports cytoskeletal reorganization for many cellular processes. This family of small GTPases is found in all eukaryotes and has been shown to regulate actin dynamics. Rho proteins act as molecular switches that cycle between an inactive GDP-bound state to an active GTP-bound state. As such, these proteins must be tightly regulated in order to prevent aberrant activation of their downstream effectors. This regulation occurs immediately after the addition of posttranslational modifications, such as farnesylation or geranylation, that position the inactive GTPase within the plasma membrane (Ridley, 2006). Inactivation is enhanced by the presence of Rho Guanine Dissociation Inhibitors (RhoGDIs), which interact with the isoprenyl GDP/GTP switch region of Rho GTPases and ultimately prevent their activation and translocation to target membranes (Hori *et al.*, 1991; Michaelson *et al.*, 2001). Signaling events, as well as dissociation factors, allow for release of Rho GTPases from RhoGDIs. Once Rho GTPases are released, they are able to interact with guanine nucleotide exchange factors (GEFs), which catalyze the exchange of GDP for GTP. This exchange activates Rho GTPases and allows them to interact with downstream effectors (Ridley *et al.*, 2003). Upon stimulus removal, Rho GTPases interact with GTPase activating proteins (GAPs), which hydrolyze GTP, and return the Rho GTP to its inactive state (Hori *et al.*, 1991). Rho GTPases play an important role in the formation of actin comet tails in this process, Rho GTPases, specifically Cdc42, activate N-WASP, which is then recruited to endosomal membranes (Bu *et al.*, 2010). Activated N-WASP can recruit Arp2/3 to nucleate actin comets (Bu *et al.*, 2010), thus serving as a propulsion force at the

endosomal membrane. Recently it was shown that RhoB is also involved in the formation of actin comets (Sandilands *et al.*, 2004). RhoB activation facilitates actin comet formation by stimulation of two classes of actin polymerization machinery, formins (mDia1, mDia2) and Arp2/3. This stimulation has a functional consequence, as the induction of actin polymerization machinery can, in turn, provide the necessary force at vesicle membranes to propel them in the cytoplasm.

Actin in vesicular trafficking

Actin is a highly conserved protein that is encoded by multiple genes within an organism. Like MTs, actin filaments exhibit a plus- to minus-end polarity, with higher monomer affinity at the plus end. Actin polymerizes as both a meshwork and as parallel bundles. These distinct actin networks are important for cell motility, either by forming lamellipodia or by providing the contractile force necessary to move the cell. The nucleation and subsequent polymerization of actin filaments is important to drive many cellular processes, including vesicular trafficking (Sandilands *et al.*, 2004). Due to its dynamic properties, actin plays various roles in the transport of endocytic vesicles; first, actin may serve as tracks for motor-driven vesicular transport. Additionally, actin promotes tubule formation and vesicle fission. Moreover, actin polymerization can occur asymmetrically at the vesicle membrane to provide a pushing force in the form of actin comets. The best characterized mechanism for Arp2/3-dependent actin comet tail formation is in the bacterium *Listeria monocytogenes*, which utilize an Arp2/3 interacting protein, *ActA,* to hijack host actin polymerization machinery (Cameron *et al.*, 1999). In eukaryotes, a similar mechanism of actin comet tail formation has been described as a

general mechanism by which endosomes are trafficked. Actin comet tail formation can also occur as a result of the activation of formins, mDia1 and mDia2 (Sandilands *et al.*, 2004). Activation of these formins localizes them to endosomal membranes where they can facilitate the polymerization of filamentous actin. This mechanism of formin-mediated vesicle delivery is one of the currently accepted hypotheses on how the proto-oncogene c-Src, whose localization and activity must be finely tuned to ensure proper signaling, is trafficked and positioned in cells.

c-Src as a proto-oncogene

Src is a major proto-oncogene that is involved in a variety of human cancers. Though Src is rarely mutated in human cancers, it has been shown to exhibit elevated expression levels to elicit oncogenic transformation (Irby and Yeatman, 2000). Src activity and localization must be tightly regulated in order to prevent aberrant signaling. Src signaling is important for a variety of cellular processes, such as cell motility and regulation of endocytosis (Sanjay *et al.*, 2001; Cao *et al.*, 2010). Src contains six domains and can be regulated in a variety of ways. In the inactive state, C-terminal Src Kinase (CSK) phosphorylates Src at Tyrosine 527, allowing Src to assume a folded conformation, which prevents phosphorylation of Tyrosine 416 within the kinase domain. Activation of Src, either through direct binding of Focal Adhesion Kinase (FAK) or dephosphorylation of Tyrosine 527 by phosphatases PTP or SHP1/2, allows Src to assume an open conformation. This open conformation then allows for phosphorylation of Src in the kinase domain by PKC (Protein Kinase C), PKA (Protein Kinase A) and other kinases, thereby permitting Src to phosphorylate downstream targets. Disruption

of Src function has been shown to cause defects in cell motility and invasion. Src knockout mice exhibit defects in tooth eruption, reproductive organ development, osteopetrosis, and T-cell development (Roby *et al.*, 2005).

Src has been shown to be transported within the cell in association with endosomal membranes (Horne *et al.*, 1992; Kaplan *et al.*, 1992; Reinecke *et al.*, 2014). However, there are currently two opposing views as to how Src may be trafficked at these endosomal membranes. While Src-associated endosomes have been shown to be trafficked bidirectionally along MTs in neurons (Wu *et al.*, 2008), another report showed that in fibroblasts Src-associated endosomes are trafficked by polymerizing actin, likely in the form of actin comet tails (Sandilands *et al.*, 2004). The trafficking of Src-associated endosomes by actin polymerization relies on the small GTPase, RhoB. Nonetheless, the precise subcellular localization of Src via trafficking is critical for Src to perform its functions, such as in signaling (Donepudi and Resh, 2008), development (Berta *et al.*, 2011), and in degradative podosome formation in osteoclasts and cancer cells (Berdeaux *et al.*, 2004; Miyazaki *et al.*, 2004; Boateng *et al.*, 2012). The underlying mechanism required to precisely position c-Src within specific cellular domains continues to be a topic of debate, but it appears that contributions by both cytoskeletal networks are possible and may potentially coordinate to improve the efficiency of the c-Src vesicle trafficking.

Mediating cytoskeletal crosstalk

MTs and actin exhibit two mechanistic classes of interactions, both regulatory and structural (Rodriguez *et al.*, 2003). During cell polarization, MT depolymerization influences the polarity of actin filaments (Rodriguez *et al.*, 2003). In addition, it has been shown in S. *cerevisiae* that capture of MT plus-ends by the EB1 ortholog, Bim1p, at the cell cortex by the Adenomatous Polyposis coli (APC) ortholog, Kar9p, is required for transport of MTs along actin filaments, their capturing at the cell cortex, and for organization of the MT cytoskeleton (Tirnauer *et al.*, 1999). Another well-characterized mechanism of crosstalk involves the Rho family of small GTPases. Specifically, RhoA promotes both the formation of actin stress fibers and the stabilization of a subset of MTs, thus coordinating actin filaments and MTs (Imamura *et al.*, 1998). Rac1, another RhoGTPase, has also been shown to regulate the polymerization of both actin and MTs (Guo *et al.*, 2006). Coordination of the MT and actin networks is also regulated by the Rho Guanine Nucleotide Exchange Factor, GEF-H1 (Krendel *et al.*, 2002), which catalyzes the exchange of GDP for GTP and the subsequent activation of Rho family class members, including RhoA and RhoB (Kamon *et al.*, 2006; Birkenfeld *et al.*, 2007; Chang *et al.*, 2008). Binding to MTs inhibits GEF-H1 activity (Yoshimura and Miki, 2011), but upon MT depolymerization, GEF-H1 assumes an active conformation, which allows it to interact with downstream targets (Yoshimura and Miki, 2011). Together, this indicates a clear connection between the cytoskeletal networks and a mutual regulation by Rho GTPases.

Thesis Summary

The work presented in this thesis follows years of investigation by other scientists into the mechanisms by which RASSF1A expression can be lost through promoter hypermethylation, as well as the overall effects on various cells types; however, the cell biological function of RASSF1A MT binding and the effects that its loss has on MT-related processes in interphase cells has yet to be examined. Additionally, the work presented here is also the product of a long-standing debate about the true mechanism of c-Src trafficking within cells, specifically, which cytoskeletal elements and proteins are involved in the process.

In Chapter II, I highlight my efforts to efforts to determine the functional consequence of RASSF1A binding to MTs. Chapter II discusses how RASSF1A localizes to MTs, as well as how this binding influences MT stabilization and protection, MT dynamics, Golgi organization and maintenance, and cell migration. Chapter III presents a second project that focuses on solving the debate on the mechanism of c-Src trafficking and identifying the molecular players involved. Overall, this thesis contributes to a better understanding of the functional significance of RASSF1A binding to MTs, in addition to, the resolution of the mechanisms involved for regulation of c-Src trafficking.

CHAPTER II

Microtubule segment stabilization by RASSF1A is required for proper microtubule dynamics and Golgi integrity

This chapter is published under the same title in *Molecular Biology of the Cell,* January, 2014 (Arnette et al., 2014).

Abstract

The tumor suppressor and microtubule-associated protein, Ras-association domain family 1A (RASSF1A), has a major impact on many cellular processes, such as cell-cycle progression and apoptosis. RASSF1A expression is frequently silenced in cancer and is associated with increased metastasis. Therefore, we tested the hypothesis that RASSF1A regulates microtubule organization and dynamics in interphase cells, as well as the impact on Golgi integrity and cell polarity. Our results show that RASSF1A utilizes a unique microtubule-binding pattern to promote site-specific microtubule rescues, and loss of RASSF1A led to decreased microtubule stability. Furthermore, RASSF1A-associated stable microtubule segments are necessary to prevent Golgi fragmentation and dispersal in cancer cells and maintain a polarized cell front. These results indicate that RASSF1A is a key regulator in the fine-tuning of microtubule dynamics in interphase cells and proper Golgi organization and cell polarity.

Introduction

Ras association domain family 1A (RASSF1A) is a tumor suppressor whose inactivation is thought to be responsible for 40 types of sporadic human cancers (van der Weyden and Adams, 2007). Recruitment of DNA methyltransferases to the RASSF1A promoter, and subsequent promoter hypermethylation, serves as the main mechanism of RASSF1A loss (Dammann *et al.*, 2000; Burbee *et al.*, 2001; Lee *et al.*, 2001). As RASSF1A lacks enzymatic function (Donninger *et al.*, 2007), the currently accepted function is to serve as a scaffold for a number of essential signaling interactions (Donninger *et al.*, 2007). Therefore, RASSF1A can participate in a variety of processes that regulate apoptosis (Vos *et al.*, 2000; Baksh *et al.*, 2005) and cell-cycle progress (Shivakumar *et al.*, 2002), both of which likely impart the tumor suppressive function of RASSF1A by decreasing the cancer cell number. Besides the scaffolding function, RASSF1A also strongly binds microtubules (MTs) *in vitro* and in cells (Dallol *et al.*, 2004). Such binding increases MT stability: in cells, RASSF1A overexpression induces MT hyper-stabilization, while RASSF1A depletion decreases MT resistance against depolymerizing drugs (Liu *et al.*, 2003; Dallol *et al.*, 2004). MT-binding ability of RASSF1A was proposed to be important for the mitotic spindle dynamics and cell cycle progression (Rong *et al.*, 2004; Vos *et al.*, 2004). Currently, it is clear that RASSF1A regulates cell cycle progression acting as an Aurora A-dependent scaffolding platform within a complex signaling mechanism (Rong *et al.*, 2007). MT binding likely contributes to this mechanism via RASSF1A recruitment (Song *et al.*, 2004; Rong *et al.*, 2007), which may be important for the tumor suppressive function RASSF1A, as mutants deficient in MT binding were not as potent in cell-cycle arrest (Dallol *et al.*, 2004).

However, there is no direct evidence for the importance of RASSF1A-dependent MT stabilization in mitosis-cell cycle regulation.

Importantly, loss of RASSF1A expression in cancer cells is concomitant with the formation of a more invasive and metastatic cancer phenotype (Lee *et al.*, 2001; Muller *et al.*, 2003; Kang *et al.*, 2004; Liu *et al.*, 2005; Jo *et al.*, 2006), which depends strongly on migratory rather than proliferative features of cancer cells. Indeed, RASSF1A depletion was shown to facilitate HeLa cell migration *in vitro* (Dallol *et al.*, 2005). It has been hypothesized that the ability of RASSF1A to bind MTs is responsible for this phenotype (Dallol *et al.*, 2004), which would have been a justified function for RASSF1A-dependent MT stabilization. Indeed, RASSF1A depletion affects the overall MT pattern(Dallol *et al.*, 2005); however, the origin of this change has not been addressed, and whether and how RASSF1A regulates MT dynamic instability in motile cells is unknown.

Here, we applied high-resolution confocal and TIRF microscopy to determine RASSF1A-dependent MT regulation in motile cells in detail. Because the function of known MT-binding proteins depends on their specific localization and dynamics within the MT network, we also investigated cellular localization of RASSF1A and potentially associated functions. We determined that RASSF1A binds to MTs in a distinct segmental pattern and exerts its MT-stabilizing effect only within these segments. Such site-specific MT stabilization increases MT rescue frequency specifically at the RASSF1A-coated MT segments. RASSF1A-associated MT segments serve as sites for

temporal bundling of short regions within MTs, which probably contributes to MT network organization. We also found that RASSF1A-associated MT segments are necessary for the Golgi complex integrity and positioning, which is a known essential determinant for polarized cell migration (Kupfer *et al.*, 1983; Miller *et al.*, 2009; Yadav *et al.*, 2009). This study provides the first evidence of the role of MT-bound RASSF1A in MT dynamic instability regulation and the architecture of interphase cells.

Results

RASSF1A localizes at discrete MT segments

The goal of this study was to investigate functions for RASSF1A in interphase cells and to determine whether loss of these functions is essential for phenotypes of cancer cell in which RASSF1A is silenced. To address this, we utilized two cells systems, including normal Retinal Pigment Epithelial cell (RPE1) and the epithelial breast cancer cell line, MCF-7. To determine RASSF1A localization and dynamics, GFP- or RFP-fused RASSF1A was ectopically expressed in both cell types, and expression levels were examined by immunoblotting. We found that endogenous expression of RASSF1A was low in RPE1, and, as previously reported (Kellokumpu *et al.*, 2002), completely absent in MCF-7. Since high expression of RASSF1A is known to over-stabilize MTs (Liu *et al.*, 2003; Dallol *et al.*, 2004; Rong *et al.*, 2004; Vos *et al.*, 2004), ectopic expression of fluorescently-fused RASSF1A in cells used for our experiments was maintained at near or slightly less than endogenous levels (Figure 2.1 A). Under these conditions, RASSF1A was detected as short linear segments (Figure 2.1 B', B'''). Because previous reports have shown that ectopically expressed RASSF1A can bind to the MT lattice (Rong *et al.*, 2004), co-localization of these segments with MTs was tested by alpha-tubulin immunostaining of RFP-RASSF1A-expressing cells. We found that RASSF1A was localized linearly along the lattice of distinct MTs, highlighting a segmental pattern within the MT network (Figure 2.1 B-B''', left cell); however, when RFP-RASSF1A was overexpressed, this segmental pattern within the MT network was lost and MT bundling occurred (Figure 2.1 B, right cell). We hypothesize that this unusual binding pattern may impart an important function for MT organization.

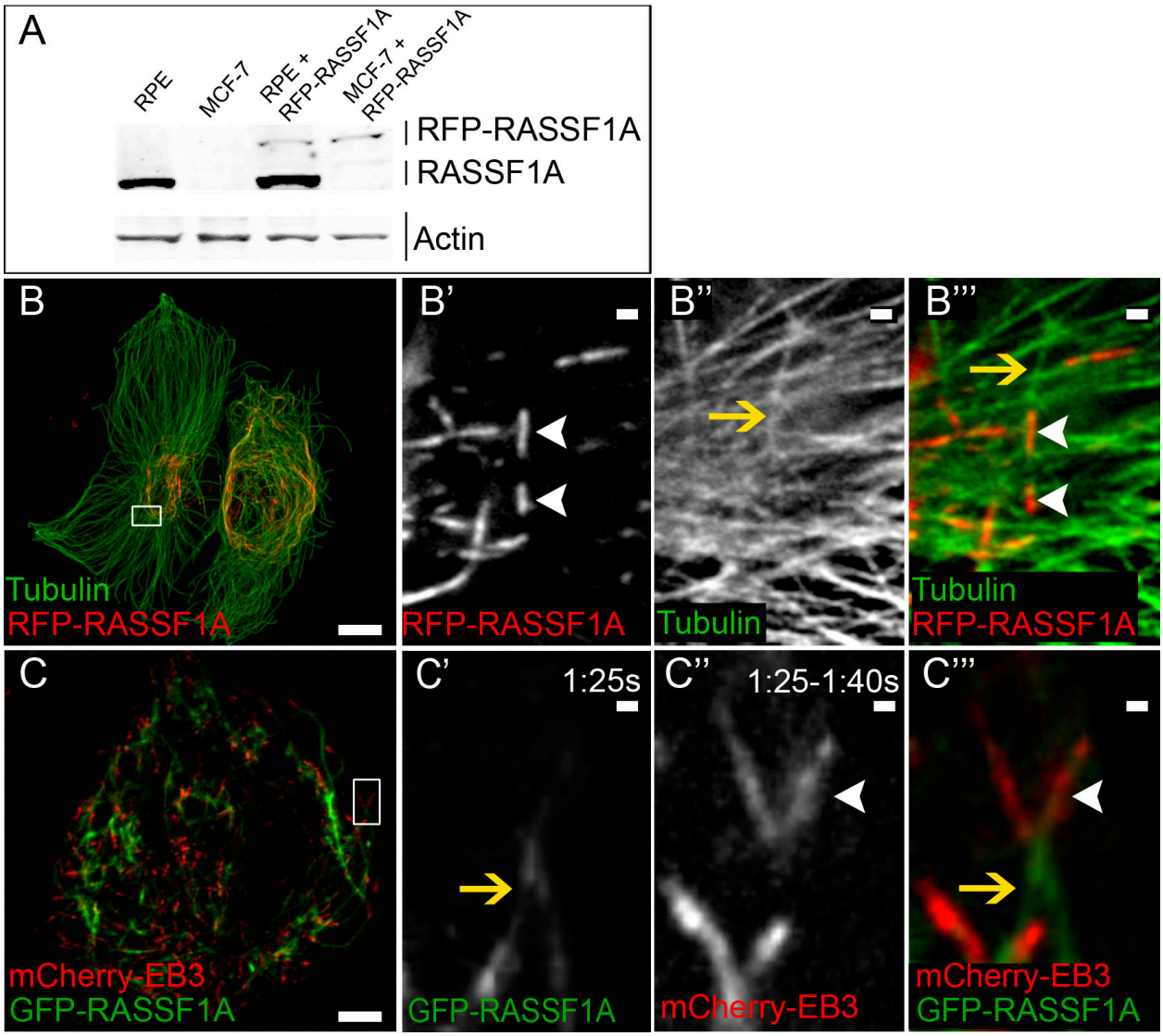
A
RPE
MCF-7
RPE + RFP-RASSF1A
MCF-7 + RFP-RASSF1A
RFP-RASSF1A
RASSF1A
Actin
B
Tubulin
RFP-RASSF1A
B'
RFP-RASSF1A
B''
Tubulin
B'''
Tubulin
RFP-RASSF1A
C
mCherry-EB3
GFP-RASSF1A
C'
1:25s
GFP-RASSF1A
C''
1:25-1:40s
mCherry-EB3
C'''
mCherry-EB3
GFP-RASSF1A

Figure 1: RASSF1A binds to the non-dynamic portion of MTs.

(A) Western blot analysis of endogenous RASSF1A (Lanes 1,2) and expressed RFP-RASSF1A (Lanes 3,4) in RPE1 and MCF-7 cells. (B) RPE1 cells expressing RFP-RASSF1A (red) fixed and stained for tubulin (green). Immunostaining. Bar, 5μm. (B'-B''') RFP-RASSF1A (white arrowheads) localizes segmentally along MTs (yellow arrow) shown in (B). Bar, 2μm. (C) Detection of GFP-RASSF1A (green) and mCherry-EB3 (red) in time-lapse TIRFM movie of a MCF-7 cell (5s/frame). Maximum intensity projection of four frames from mCherry-EB3 channel illustrates polymerizing MT plus end (C"). Bar, 5μm. (C'-C''') GFP-RASSF1A does not colocalize with mCherry-EB3 at the tip of MTs shown in *C.* Bar, 2μm.

Binding of RASS1A locally stabilizes MT segments

Because localization of dynamic versus stable MTs defines the configuration of trafficking paths within a cell, and thus, is tightly connected with MT function, we addressed whether RASSF1A locally stabilizes MT segments. To determine whether RASSF1A-associated MT segments were dynamic, we applied live-cell total internal reflection fluorescence (TIRF) imaging of cells co-expressing GFP-RASSF1A and a MT plus-tip marker, mCherry-EB3. Polymerizing MTs, detected by tracking of EB3 comets, were devoid of RASSF1A. In many cases, RASSF1A was found at the non-dynamic portions of MTs, away from the plus ends undergoing dynamic instability (Figure 2.1 C-C’’’).

These data suggest that RASSF1A associates with specific, non-dynamic regions of dynamic MTs away from the polymerizing plus ends. To test whether binding of RASSF1A extends lifetimes of distinct regions of MTs, we addressed if these MT portions were post-translationally modified. As detyrosination (Glu Tubulin) is an established marker for long-lived MTs, we first tested for this PTM by immunostaining in RPE1 cells transiently expressing variable levels of RFP-RASSF1A. Non-transfected cells exhibited low Glu tubulin levels (Figure 2.2 A-D). We detected enhanced levels of Glu tubulin in cells expressing RFP-RASSF1A (Figure 2.2 E-G’’, D), where these levels correlated with the level of RASSF1A expression (Figure 2.2 D). On a single MT level, Glu-tubulin was either co-localized with RASSF1A, or accumulated at MT regions flanked by RASSF1A-coated segments (Figure 2.2 G’-G’’), indicating that RASSF1A facilitated tubulin detyrosination indirectly by increasing MT lifetimes. We also found that

RASSF1A-associated MTs were often acetylated, though tubulin acetylation did not correlate with RASSF1A expression (not shown), indicating that though over-stabilized MTs accumulate tubulin acetylation (Piperno *et al.*, 1987; Westermann and Weber, 2003), other molecules are likely responsible for specific MT acetylation in cells. To examine whether RASSF1A-associated MT regions were indeed stabilized against depolymerization, RPE1 cells expressing RFP-RASSF1A and 3x-GFP-EMTB (ensconsin MT binding domain (Faire *et al.*, 1999; Tanaka *et al.*, 2009)), were subjected to the MT-depolymerizing agent, nocodazole. Confocal live-cell imaging revealed that MT depolymerization proceeds up to the point where RASSF1A is associated with the MT (Figure 2.2 H-J), indicating that RASSF1A locally protects the MT from further depolymerization. Thus, RASSF1A-coated MT segments might serve to regulate site-specific MT dynamics.

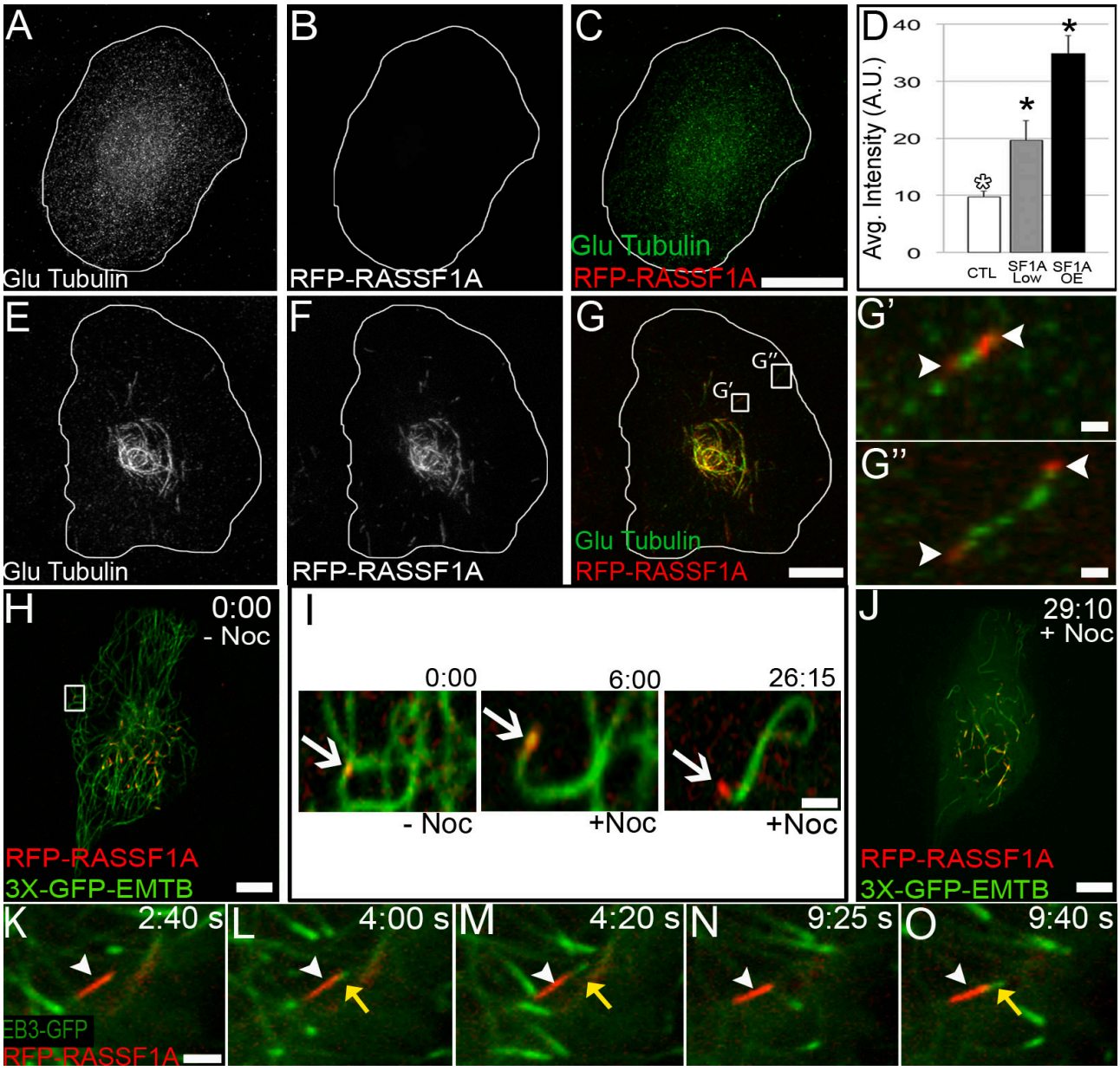
A
Glu Tubulin
B
RFP-RASSF1A
C
Glu Tubulin
RFP-RASSF1A
D
Avg. Intensity (A.U.)
40
30
20
10
0
CTL
SF1A Low
SF1A OE
E
Glu Tubulin
F
RFP-RASSF1A
G
G''
G'
Glu Tubulin
RFP-RASSF1A
G'
G''
H
0:00
- Noc
RFP-RASSF1A
3X-GFP-EMTB
I
0:00
6:00
26:15
- Noc
+Noc
+Noc
J
29:10
+ Noc
RFP-RASSF1A
3X-GFP-EMTB
K
2:40 s
EB3-GFP
RFP-RASSF1A
L
4:00 s
M
4:20 s
N
9:25 s
O
9:40 s

Figure 2.2: RASSF1A binding stabilizes and protects MTs from depolymerization.

(A-C) Non-transfected RPE1 cell does not exhibit detyrosinated (green) MTs in the absence of RFP-RASSF1A (red) expression. Immunostaining. (D) Intensity of detyrosinated (Glu) tubulin as correlated with RFP-RASSF1A expression. Representative examples out of 20 cells/condition. Error bars indicate s.e.m. (E-G) RFP-RASSF1A expression induces MT stabilization in RPE1 cells as detected by anti-detyrosinated (Glu) tubulin staining. Immunostaining. Bar, 5μm. (G'-G'') RFP-RASSF1A (red; white arrowheads) flanks portions of stable MTs as detected by anti-detyrosinated (Glu) tubulin staining shown in *G*. Immunostaining. Bar, 2μm. (H and J) Video frames of RFP-RASSF1A (red) and 3x-GFP-EMTB (green) expressing cells representing pre- and post-nocodazole treatment. Spinning-disk confocal (5s/frames). (I) Time sequences pre- and post-nocodazole addition illustrates RFP-RASSF1A (white arrow) MT protection capacity. Bar, 5μm. (K-O) RFP-RASSF1A (red; white arrowhead) expression in RPE1 cells can function as sites of MT rescue, as detected by EB3-GFP labeled growing MT plus-ends (green; yellow arrow). Spinning-disk confocal (5s/frames). Bar, 5μm.

RASSF1A localization defines sites of MT rescues

As RASSF1A binds segmentally to the MT lattice, one can infer that the segment borders provide distinct points of stabilization, which could serve as platforms for switching of MTs from depolymerization to polymerization (MT rescues). The location and persistence of rescue sites at interphase MTs, which continuously undergo dynamic instability, is crucial for MT network configuration. However, although RASSF1A has been implicated in influencing MT dynamics in mitosis (Vos *et al.*, 2004), the direct effects of RASSF1A on MT dynamics in interphase have not been addressed. To investigate the potential involvement of RASSF1A in regulating interphase MT dynamics, steady state analysis of RPE1 cells co-expressing low levels of RFP-RASSF1A and EB3-GFP was performed. Cells were imaged with a spinning-disk confocal microscope to monitor the plus ends of growing MTs. RASSF1A-associated MTs acted as platforms for polymerizing MTs (Figure 2.2 K-O), which suggests that these sites can serve as points of rescue. To analyze the role of endogenous RASSF1A in overall MT dynamics parameters, peripheral MT dynamics were analyzed in H1792 cells, a non-small cell lung carcinoma cell line, either expressing endogenous RASSF1A or shRNA depleted of RASSF1A (Figure 2.3 A) (Vos *et al.*, 2006) by TIRF microscopy. Loss of RASSF1A via shRNA knockdown resulted in alterations in MT organization as compared to RASSF1A expressing cells (Figure 2.3 B-C). Consistent with our model, we found that the number of rescue events (Figure 2.3 D) and pause duration (Figure 2.3 E) per MT was significantly decreased by RASSF1A depletion, indicating that this protein indeed functions as a rescue factor by stabilizing MT segments. Additionally, our analyses revealed that RASSF1A depletion led to an increase of MT polymerization and

depolymerization rates (Figure 2.3 G-H), as well as catastrophes per MT (Figure 2.3F). Such enhancement of MT dynamicity could be a manifestation of a lack of short-term pauses and rescues and is characteristic for depletion of a rescue factor (Mimori-Kiyosue *et al.*, 2005; Drabek *et al.*, 2006). Collectively, these alterations in dynamics strongly decreased MT lifetimes after RASSF1A depletion (Figure 2.3 I-J).

Taken together, our data suggests a critical role for RASSF1A in fine tuning interphase MT network dynamics.

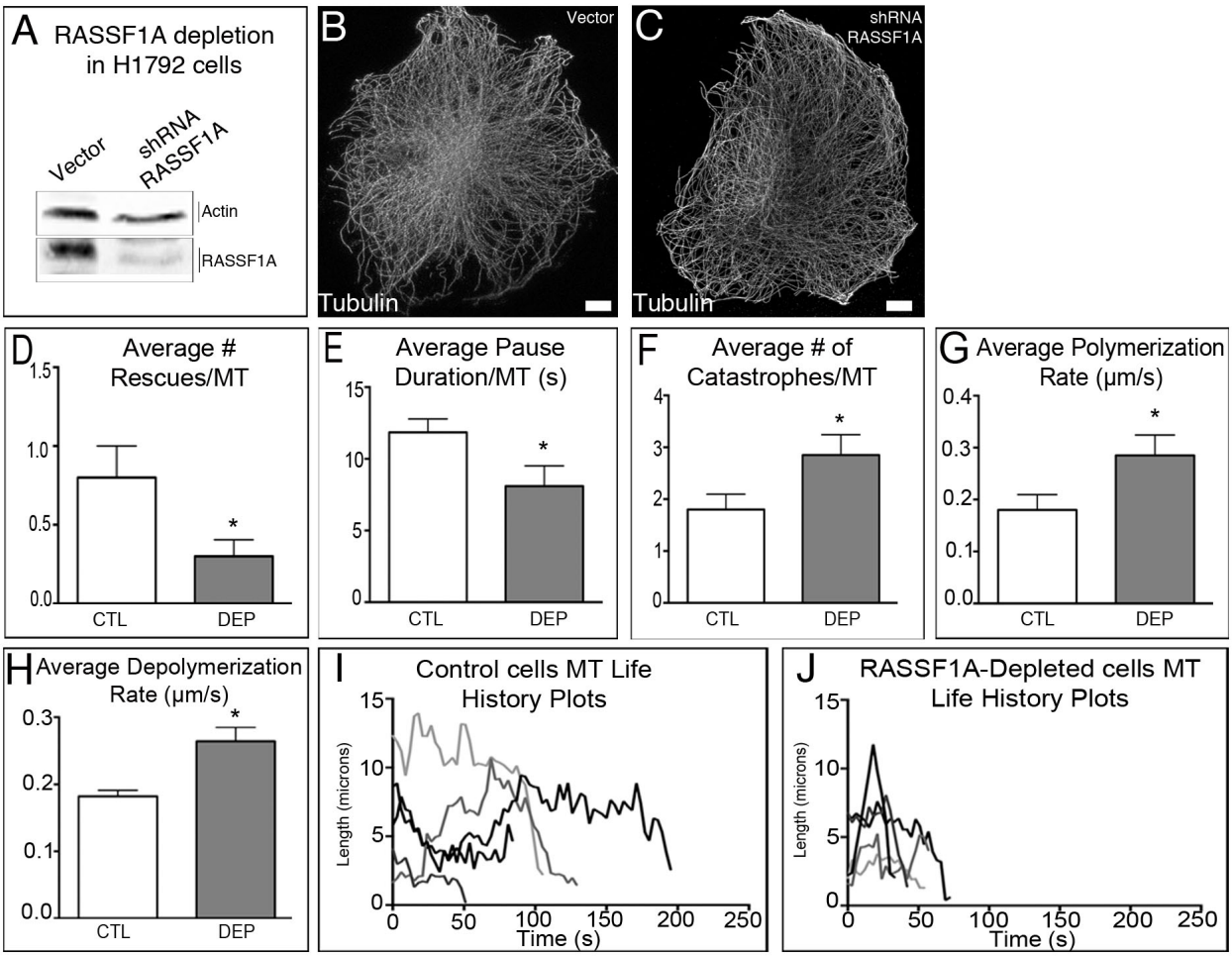
A RASSF1A depletion in H1792 cells
Vector
shRNA RASSF1A
Actin
RASSF1A
B
Vector
Tubulin
C
shRNA RASSF1A
Tubulin
D Average # Rescues/MT
1.5
1.0
0.5
0.0
CTL
DEP
E Average Pause Duration/MT (s)
15
10
5
0
CTL
DEP
F Average # of Catastrophes/MT
4
3
2
1
0
CTL
DEP
G Average Polymerization Rate (μm/s)
0.4
0.3
0.2
0.1
0.0
CTL
DEP
H Average Depolymerization Rate (μm/s)
0.3
0.2
0.1
0.0
CTL
DEP
I Control cells MT Life History Plots
Length (microns)
15
10
5
0
0
50
100
150
200
250
Time (s)
J RASSF1A-Depleted cells MT Life History Plots
Length (microns)
15
10
5
0
0
50
100
150
200
250
Time (s)

Figure 2.3: RASSF1A depletion influences MT dynamics.

(A) Western blot analysis of RASSF1A in vector expressing (Lane 1) and RASSF1A shRNA depleted (Lane 2) H1792 cells. (B-C) H1792 cells expressing vector (B) or RASSF1A shRNA depleted (C) fixed and immunostained for tubulin. Immunostaining. Bar, 5μm. (D-J) Analysis of various MT dynamics parameters in H1792 RASSF1A shRNA depleted cells, reveals an increase in MT dynamicity. *p-value* < .05. Error bars indicate s.e.m. (I-J), Examples of MT life history plots in control H1792 cells and cells depleted of RASSF1A. Plots reveal decreased MT lifetimes upon RASSF1A depletion. Representative examples out of 20 cells/condition.

RASSF1A bundles neighboring MTs

Because RASSF1A-associated MT segments clearly bear a specialized function in local MT behavior, we next addressed their positioning and integration within the whole MT network. We hypothesized that if RASSF1A were stably bound to MTs, addition of nocodazole would not increase cytoplasmic RFP-RASSF1A levels. Confocal live-cell imaging under these conditions revealed no appreciable increase in cytoplasmic RFP-RASSF1A levels, and instead RFP-RASSF1A remained associated with MT fragments (compare a pre-nocodazole cytoplasmic fluorescence intensity of 176952 a.u. to a post-nocodazole intensity of 183031 a.u., no significance). FRAP analysis also revealed that RFP-RASS1A is non-dynamic, suggesting that it is stably associated with a MT (Figure 2.S1). Further analysis of live-cell imaging sequences showed that RASSF1A could promote bundling of pre-existing steady-state MTs (Figure 2.4 A-B'''; 2.S2). MT bundling often resulted in a change in MT directionality from random to parallel, and coincided with the formation of thin MT bundles. Fluorescence intensity analysis of 3x-GFP-EMTB labeled MTs revealed that on average there is a three-fold increase in EMTB signal for RASSF1A-associated segments as compared to single MTs not bound by RASSF1A (Figure 2.4 C), suggesting that RASSF1A can bundle up to three MTs. Quantification of non-RASSF1A-associated MT bundling events in 1.5μm^2 squares (similar to the size of RASSF1A segments), and RASSF1A-associated MTs revealed that the majority of RASSF1A-coated MT segments facilitate bundling within the MT network (Figure 2.4 D). Additionally, quantification of non-RASSF1A-associated MT unbundling reveals a significantly higher number of unbundling events as compared to RASSF1A-associated MTs (Figure 2.4 E). Thus, RASSF1A stabilizes MT-MT interactions, which could provide

a significant influence in altering the MT network configuration. These properties can be used for specific MT functions required at distinct cellular locations. For example, centrally located RASSF1A-associated segments may facilitate reliable Golgi complex assembly (Ryan *et al.*, 2012) by maintaining the Golgi complex integrity (Cole *et al.*, 1996).

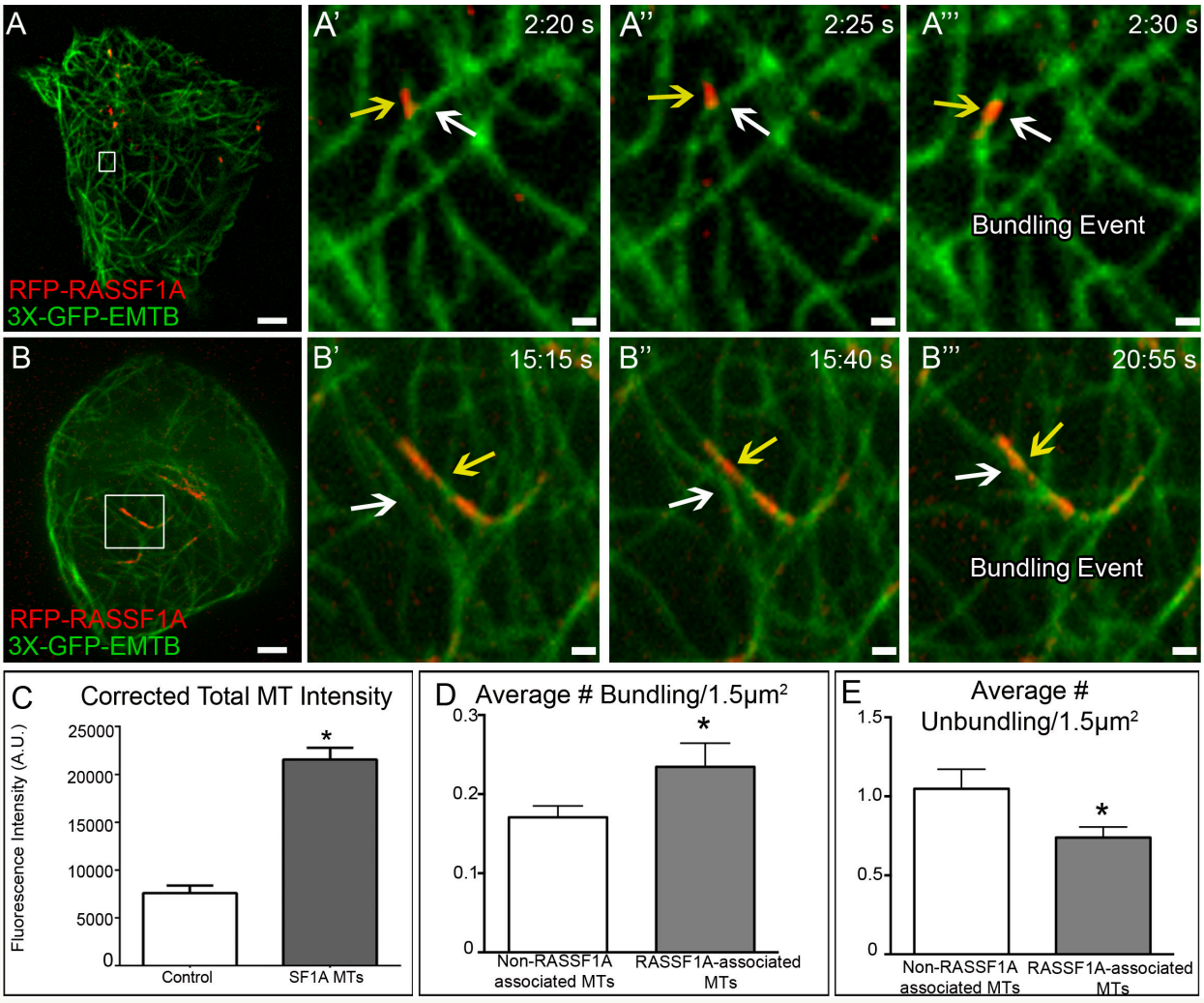
A
A'
2:20 s
A''
2:25 s
A'''
2:30 s
Bundling Event
RFP-RASSF1A
3X-GFP-EMTB
B
B'
15:15 s
B''
15:40 s
B'''
20:55 s
Bundling Event
RFP-RASSF1A
3X-GFP-EMTB
C
Corrected Total MT Intensity
Fluorescence Intensity (A.U.)
25000
20000
15000
10000
5000
0
*
Control
SF1A MTs
D
Average # Bundling/1.5μm²
0.3
0.2
0.1
0
*
Non-RASSF1A associated MTs
RASSF1A-associated MTs
E
Average # Unbundling/1.5μm²
1.5
1.0
0.5
0
*
Non-RASSF1A associated MTs
RASSF1A-associated MTs

Figure 2.4: RASSF1A is transported with MTs and induces local bundling to alter MT network configuration.

(A and B) RPE1 cells expressing RFP-RASSF1A and 3X-GFP-EMTB. Area in box is enlarged to the right. Spinning-disk confocal. Bar, 5μm (A'-A''' and B'-B''') RFP-RASSF1A (yellow arrow) locally bundles neighboring MTs (white arrow). Bar, 2μm. (C) Analysis of fluorescence intensity in single versus RASSF1A-associated MTs reveals RASSF1A can bundle at least 3 MTs at one time. Representative examples out of 15 cells/condition. Error bars indicate s.e.m. (D) Average number of bundling events per $1.5\mu m^2$ reveals a significant increase in these events with RASSF1A-associated MTs as compared to non-RASSF1A-associated MTs. (E) Average number of unbundling events per $1.5\mu m^2$ reveals a significant decrease in unbundling events in RASSF1A-associated MTs as compared with non-RASSF1A-associated MTs. Representative examples out of 10 cells.

RASSF1A-associated MT segments are required for Golgi integrity

Analysis of the cellular localization of RASSF1A-associated MT segments revealed that they were accumulated predominantly in the central cell region. Co-staining with a Golgi marker, GM130, revealed the close proximity of these segments with the Golgi apparatus (Figure 2.5 A-C). Such specific localization may indicate that MTs in the Golgi area possess higher RASSF1A-binding properties; for example, because a cofactor needed for this segmental binding is enriched at the Golgi membrane or in the perinuclear region (e.g. the nuclear transport regulator small GTPase Ran, which was identified as a possible cofactor for MT binding of RASSF1A (Dallol *et al.*, 2004; Dallol *et al.*, 2009).) Another attractive possibility is that such localization reflects specific functions of RASSF1A-associated MTs in Golgi organization or positioning. We hypothesize that RASSF1A localization at the Golgi suggests a functional relationship whereby RASSF1A-induced MT stabilization provides a scaffold for Golgi assembly. Indeed, in MCF-7 breast cancers cells, which lack endogenous expression of RASSF1A, Golgi stacks are dispersed throughout the cell (Kellokumpu *et al.*, 2002), (Figure 5 D-F, M). To determine the role of RASSF1A in Golgi positioning, we examined the effects of altering RASSF1A protein levels on the cellular distribution of the Golgi, visualized by GM130 immunostaining. First, we utilized re-expression of RFP-RASSF1A in MCF-7 cells at low levels, which we consider close to physiological expression in non-cancerous cells (Figure 2.1 A). Interestingly, we found that under these low-expression conditions, the typically dispersed Golgi fragments were collected to the cell center (Figure 2.5 G-I, M), and the number of Golgi fragments was significantly reduced as compared to non-transfected cells (Figure 2.5N).

However, when RFP-RASSF1A was over-expressed at high levels in MCF-7 cells, resulting in coating of the entire MT network, the Golgi became redistributed throughout the cell, resembling non-transfected controls (Figure 2.5 J-L, M). This result suggests that low levels of RASSF1A, when it functions to stabilizes discrete MT segments, are necessary for proper Golgi assembly. To further test this hypothesis, we addressed if RASSF1A depletion in non-cancerous cells also affects Golgi structure. In RPE1 cells treated with either siRNA against human RASSF1A or with control scrambled siRNA (Figure 2.5 O), we determined the effect of RASSF1A depletion on Golgi structure by examining individual cells stained with GM130. In scramble control cells, the Golgi showed a compact morphology (Figure 2.5 P). In contrast, RASSF1A-depleted cells showed aberrant Golgi features, including fragmentation of the Golgi (Figure 2.5 Q-S). Interestingly, the level of Golgi fragmentation in RASSF1A siRNA depleted RPE1 cells was similar to levels observed in non-transfected or RFP-RASSF1A overexpressing MCF-7 cells (Figure 2.5 N, T). Therefore, we conclude that centrally located RASSF1A is essential for proper Golgi complex organization.

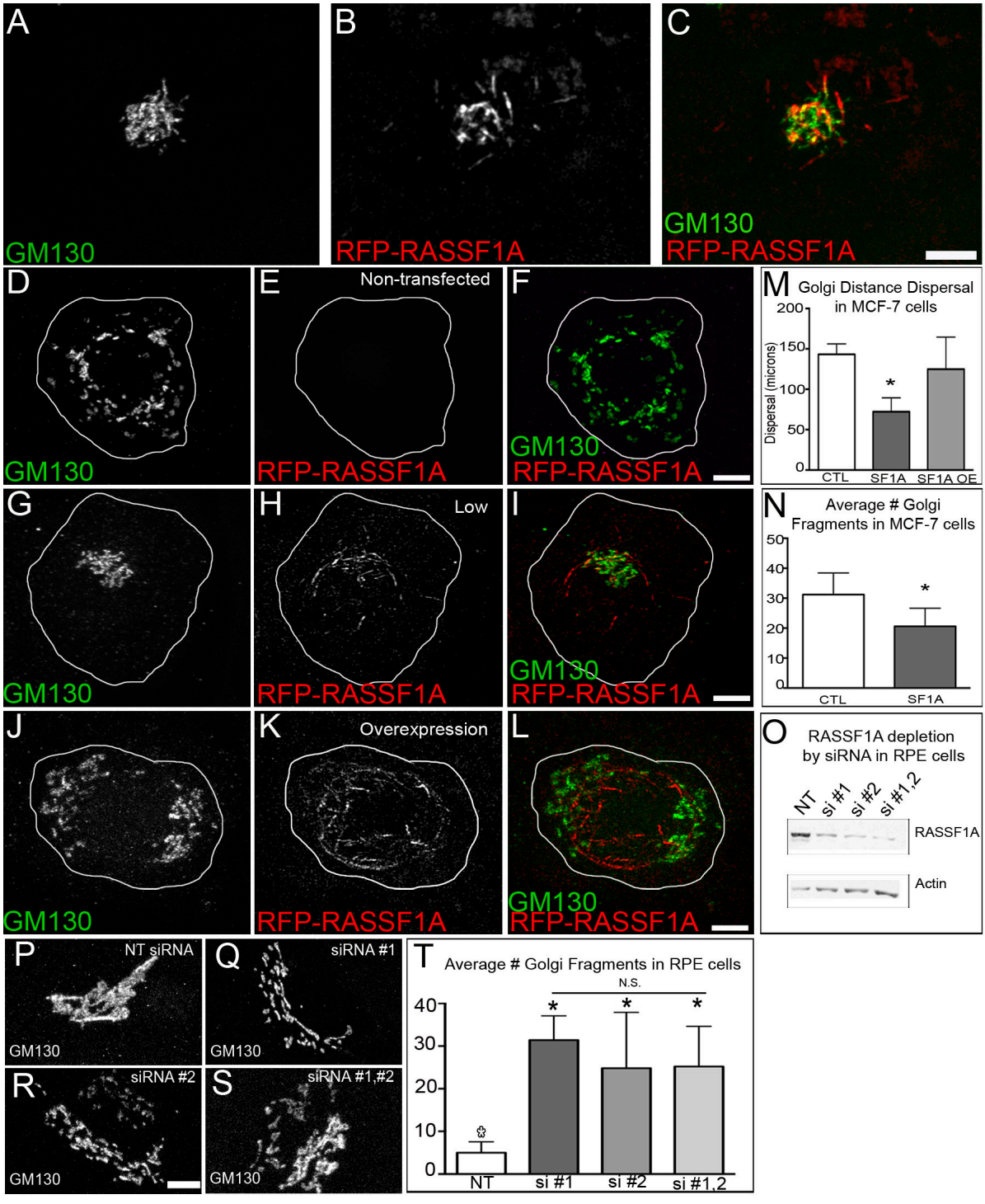
A
GM130
B
RFP-RASSF1A
C
GM130
RFP-RASSF1A
D
GM130
E
Non-transfected
RFP-RASSF1A
F
GM130
RFP-RASSF1A
M
Golgi Distance Dispersal in MCF-7 cells
Dispersal (microns)
200
150
100
50
0
*
CTL
SF1A
SF1A OE
G
GM130
H
Low
RFP-RASSF1A
I
GM130
RFP-RASSF1A
N
Average # Golgi Fragments in MCF-7 cells
50
40
30
20
10
0
*
CTL
SF1A
J
GM130
K
Overexpression
RFP-RASSF1A
L
GM130
RFP-RASSF1A
O
RASSF1A depletion by siRNA in RPE cells
NT
si #1
si #2
si #1,2
RASSF1A
Actin
P
NT siRNA
GM130
Q
siRNA #1
GM130
R
siRNA #2
GM130
S
siRNA #1,#2
GM130
T
Average # Golgi Fragments in RPE cells
N.S.
40
30
20
10
0
*
*
*
NT
si #1
si #2
si #1,2

Figure 2.5: **RASSF1A expression alters Golgi morphology.**

(A-C) MCF-7 cell expressing low levels of RFP-RASSF1A, fixed and stained for Golgi protein, GM130 (green). Immunostaining. RFP-RASSF1A localizes at MTs associated with the Golgi and at the cell periphery. (D-L) MCF-7 cells expressing various levels of RFP-RASSF1A (red) and immunostained for Golgi protein, GM130 (green). (D-F) Non-transfected MCF-7 cell exhibits a dispersed and fragmented Golgi. (G-I) MCF-7 cell expressing low levels of RFP-RASSF1A exhibits a compact Golgi. (J-L) MCF-7 cell overexpressing RFP-RASSF1A exhibits a dispersed and fragmented Golgi. Bar, 5μm. (M) Analysis of Golgi dispersal under various conditions of RFP-RASSF1A expression. Representative examples out of 10 cells/condition. (N) Analysis of Golgi fragmentation in non-transfected and low RFP-RASSF1A expressing MCF-7 cells. Representative examples out of 10 cells/condition. (O) Western blot analysis of RASSF1A siRNA depletion in RPE1 cells. Lane 1, Non-targeted (NT) RASSF1A siRNA; Lanes 2-4, RASSF1A siRNA combinations. (P-S) RPE1 cells treated with RASSF1A siRNA and immunostained for Golgi protein, GM130. (T) Analysis of Golgi fragmentation in RPE1 cells after RASSF1A siRNA depletion. Bar, 5μm. (L,M.T). Representative examples out of 10 cells/condition. Error bars indicate s.e.m.

RASSF1A-depletion disrupts cell polarity and migration

As loss of RASSF1A alters MT dynamics and Golgi organization, one can hypothesize that this loss would also impact cell migration. Previous reports have identified that RASSF1A overexpression can suppress cell migration (Dallol *et al.*, 2005; Jung *et al.*, 2013); however, the ability of low levels of RASSF1A expression to influence directionality of cell migration or polarization of migrating cells, has yet to be examined. To address the effect on directional persistence of migration, control or RASSF1A-depleted RPE1 cells were examined by differential interference contrast (DIC) microscopy and were subjected to persistence analysis. Depletion of RASSF1A significantly decreased the directional persistence of RPE1 cells (Figure 2.6 A-C), indicating that RASSF1A, likely through modulation of Golgi integrity, promotes persistent migration. Cell polarity has been analyzed assessing direction of cell protrusions formed throughout a time sequence. Area taken by all the protrusions was combined, and the circularity of the resulting shape was quantified. In this analysis, if protrusions were formed equally around the cell perimeter (lack of polarity), the overlaid protrusion area formed a donut shape (circularity equals one). If protrusions form only at one side of a cell (high polarity), the overlaid area is significantly asymmetric (circularity approaches zero). This analysis reveals a significant increase in protrusion circularity when cells were depleted of RASSF1A (Figure 2.6 D-I, J). MCF-7 cells also exhibited high measures of protrusion circularity similar to siRNA RASSF1A-depleted RPE1 cells (Figure 2.6 K-M, Q). Re-expression of RFP-RASSF1A in MCF-7 cells significantly reduced the protrusion circularity (Figure 2.6 N-P, Q; Figure 2.S3), but was unable to completely restore polarity in these cells, which may require additional molecular

players, which are inactive in these immobile cells. Additionally, re-expression of RFP-RASSF1A did not appear to influence the overall migratory ability of MCF-7 cells. Furthermore, upon re-expression of RFP-RASSF1A in MD-MBA-231 cells, a highly motile cell type, polarity was restored to levels seen in control RPE1 cells (Figure 2.6 R-W, X; Figure 2.S3) and these cells exhibited increased directional persistence (Figure 2.6 Y-A'). Thus, these data suggest that the variation in RASSF1A regulation of cell polarity may greatly depend on the inherent motile capacity within cells types. Collectively, these data suggest that RASSF1A regulation of cell polarity can potentially occur through modulation of Golgi integrity and organization, as well as via regulation of MT dynamics.

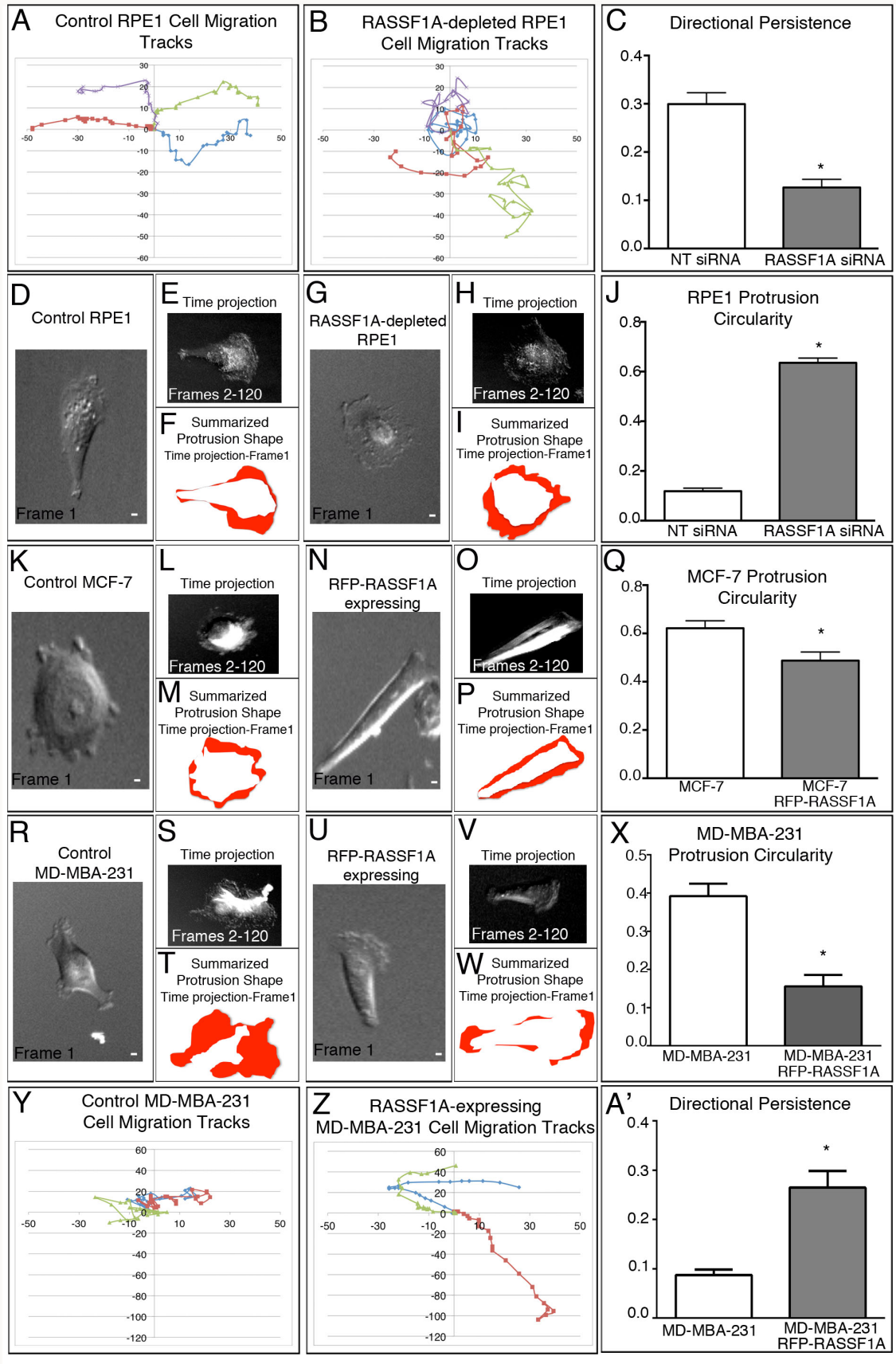
A
Control RPE1 Cell Migration Tracks
B
RASSF1A-depleted RPE1 Cell Migration Tracks
C
Directional Persistence
NT siRNA
RASSF1A siRNA
D
Control RPE1
Frame 1
E
Time projection
Frames 2-120
F
Summarized Protrusion Shape
Time projection-Frame1
G
RASSF1A-depleted RPE1
Frame 1
H
Time projection
Frames 2-120
I
Summarized Protrusion Shape
Time projection-Frame1
J
RPE1 Protrusion Circularity
NT siRNA
RASSF1A siRNA
K
Control MCF-7
Frame 1
L
Time projection
Frames 2-120
M
Summarized Protrusion Shape
Time projection-Frame1
N
RFP-RASSF1A expressing
Frame 1
O
Time projection
Frames 2-120
P
Summarized Protrusion Shape
Time projection-Frame1
Q
MCF-7 Protrusion Circularity
MCF-7
MCF-7 RFP-RASSF1A
R
Control MD-MBA-231
Frame 1
S
Time projection
Frames 2-120
T
Summarized Protrusion Shape
Time projection-Frame1
U
RFP-RASSF1A expressing
Frame 1
V
Time projection
Frames 2-120
W
Summarized Protrusion Shape
Time projection-Frame1
X
MD-MBA-231 Protrusion Circularity
MD-MBA-231
MD-MBA-231 RFP-RASSF1A
Y
Control MD-MBA-231 Cell Migration Tracks
Z
RASSF1A-expressing MD-MBA-231 Cell Migration Tracks
A'
Directional Persistence
MD-MBA-231
MD-MBA-231 RFP-RASSF1A

Figure 2.6: **RASSF1A expression and depletion disrupts directional persistence and cell polarity**.

(A-B) Representative migration tracks from control and RASSF1A-depleted RPE1. (C) Analysis of directional persistence in control and RASSF1A depleted RPE1 cells reveals that depleted cells fail to migrate directionally and exhibit more random movement. Representative examples out of 10 cells/condition. (D-I) RASSF1A-depleted RPE1 cells demonstrate a lack of polarity as compared with control RPE1. (J) Analysis of protrusion circularity in control and RASSF1A-depleted RPE1 cells. Representative examples out of 12 cells/condition. (K-P) Re-expression of RFP-RASSF1A in MCF-7 cells partially rescues cell polarity defects. (Q) Analysis of protrusion circularity in control and RFP-RASSF1A expressing MCF-7 cells. Representative examples out of 12 cells/condition. (R-W) Re-expression of RFP-RASSF1A in MD-MBA-231 cells significantly reduces the protrusion circularity. (X) Analysis of protrusion circularity in control and RFP-RASSF1A expressing MD-MBA-231. Representative examples out of 12 cells/condition. (Y-Z) Migration tracks from control and RFP-RASSF1A expressing MD-MBA-231 cells indicate an increase in directional persistence upon RASSF1A re-expression. (A') Analysis of directional persistence in MD-MBA-231 cells. Representative examples out of 12 cells/condition.

Discussion

In this study, we detected segmental binding of RASSF1A to MTs, which is an unusual pattern for a MT-associated protein. The mechanism whereby RASSSF1A accumulates at selected regions of the MT lattice may be a consequence of cooperative binding of RASSF1A molecules to a MT. Indeed, previously described ability of RASSF1A for self-association (Ortiz-Vega *et al.*, 2002), as well as for heterodimerization with other RASSF family members (Ortiz-Vega *et al.*, 2002; Praskova *et al.*, 2004; Guo *et al.*, 2007) may promote the cooperative binding. Alternatively, a preferred RASSF1A-binding area may exist within an MT, either due to accumulation of a RASSF1A-binding MT-associated protein (e.g. MAP1B (Dallol *et al.*, 2005)), or if modification of tubulin within the MT lattice favors association with RASSF1A. The latter possibility is less likely as indicated by our data (Figure 2.2). Any of these mechanisms likely leads to a high concentration of RASSF1A molecules on the MT lattice. Thus, these short regions of MT length likely exhibit properties similar to extremely stable MTs previously described in cells overexpressing RASSF1A (Liu *et al.*, 2003; van der Weyden *et al.*, 2005). On one hand, the capacity to stabilize MTs as the result of MT lattice-binding proteins is very common; many MT-associated proteins (MAPs), such as neuronal Tau (Tanaka *et al.*, 2009) or MAP2 (Takemura *et al.*, 1992) and MAP4 (Nguyen *et al.*, 1997) stabilize MTs to build long, reliable tracks for MT-dependent transport. On the other hand, the unusual segmental pattern observed with RASSF1A-driven stabilization of short MT portions provides a mechanism for distinguishing two contrasting dynamic behaviors within one MT, and serves to regulate site-specific MT dynamics.

Furthermore, our data on MT bundling indicate that massive MT bundling previously observed upon RASSF1A over-expression (Liu *et al.*, 2003; El-Kalla *et al.*, 2010) is not a random artifact but an exaggerated manifestation of a bona fide function. This evidence places RASSF1A within a subset of MAPs that contain MT bundling abilities (e.g. PRC1 (Mollinari *et al.*, 2002), Synapsin I (Baines and Bennett, 1986). Such properties likely indicate that RASSF1A is capable of remodeling the interphase MT network via local bundling and connection of short fragments among two or three MTs. RASSF1A-associated segments found close to the cell periphery, which can be revealed by TIRF microscopy (and thus proximal to the ventral cell surface), might be involved in the formation of bundled MT arrays, which may serve for directional post-Golgi trafficking towards the cell front in motile cells (Rahkila *et al.*, 1997; Schmoranzer and Simon, 2003; Lee *et al.*, 2009).

At the same time, we show that centrally located RASSF1A-associated segments facilitate Golgi complex assembly and integrity. We hypothesize that RASSF1A defines the sites of preferred Golgi interaction with MTs, and that association of RASSF1A with MT fragments in the cell center promotes Golgi stack fusion and Golgi complex integrity. In this scenario, extending RASSF1A association over the whole MT network results in scattering of these sites throughout the cell. The connection between the Golgi and MTs may be mediated either directly through RASSF1A (or some yet unidentified linker protein) binding to the Golgi components, or through creating MT sites capable of stronger molecular motor binding. Alternatively, it is also possible that RASSF1A affects Golgi organization indirectly via MT stabilization specifically within the Golgi region,

providing a long-lived platform for Golgi assembly, or by facilitation of molecular motor binding (Cai *et al.*, 2009). Furthermore, it was previously proposed that acetylation, a robust tubulin PTM found within the Golgi region, is important for MT-dependent Golgi assembly (Thyberg and Moskalewski, 1993; Ryan *et al.*, 2012). MT acetylation may contribute to a RASSF1A-dependent mechanism of Golgi assembly, but is not likely to be the whole mechanism because tubulin acetylation was found, in many cases, to be independent of RASSF1A binding to MTs (data not shown). Ultimately, we can infer that a disruption in the Golgi structure, by loss of RASSF1A, specifically interferes with other MT-dependent processes at the Golgi, such as post-Golgi trafficking.

Additionally, we show that loss of RASSF1A leads to defects in cell migration and polarity; re-expression of RASSF1A can partially rescue polarization defects. We hypothesize that loss of RASSF1A at the Golgi significantly compromises the integrity and organization of the Golgi structure, both of which are required for directional cell migration and polarization (Bershadsky and Futerman, 1994; Yadav *et al.*, 2009). With this idea, loss of RASSF1A would lead to scattering of Golgi membranes throughout the cell and the inability to form a single protrusion, potentially due to lack of directed secretion (Yadav *et al.*, 2009). Moreover, lack of the bundling capacity exerted by RASSF1A may fail to provide the necessary stable MT tracks needed to establish a polarized front (Manneville *et al.*, 2010; Chen *et al.*, 2013). Alternatively, or additionally, RASSF1A-mediated regulation of cell migration and polarity may be a result of altered MT dynamics and organization. Ultimately, we can infer that perturbations to RASSF1A levels can result in significant changes in cell morphology and behavior

Collectively, our results strongly suggest a role for RASSF1A in influencing interphase MT dynamics and Golgi positioning (Figure 2.7 A). These functions probably contribute to prevent such cancer phenotype features as disorganized cell migration, which was shown to arise from the loss of RASSF1A (Dallol *et al.*, 2005). In particular, precise spatial regulation of MT dynamics in migrating cells is necessary for maintenance of persistent lamella at the cells front (Waterman-Storer *et al.*, 1999), contact inhibition of migration (Kadir *et al.*, 2011) and asymmetric focal adhesion turnover (Kaverina *et al.*, 1999). Moreover, an integral polarized Golgi complex in the cell center is necessary for directional post-Golgi-trafficking to the cell front and directional cell migration (Yadav *et al.*, 2009). Our finding allows us to hypothesize that an established dependence of directional cell migration on RASSF1A arises from the spatial regulation of the MT network and Golgi organization by RASSF1A-associated MT segments (Figure 2.7 B)

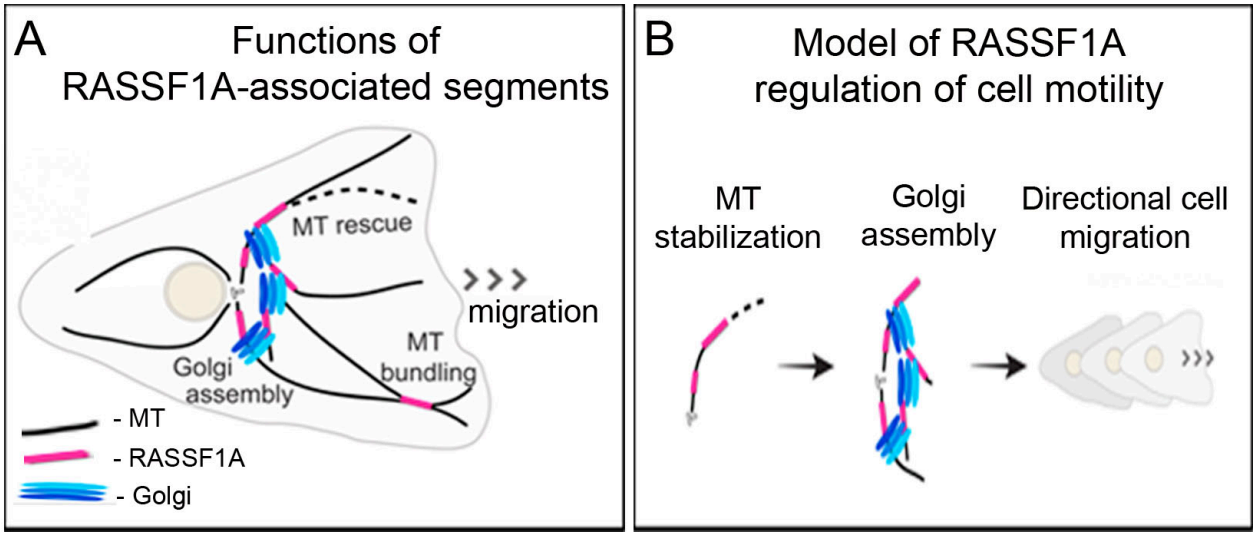
A
Functions of
RASSF1A-associated segments
MT rescue
migration
MT
bundling
Golgi
assembly
- MT
- RASSF1A
- Golgi
B
Model of RASSF1A
regulation of cell motility
MT
stabilization
Golgi
assembly
Directional cell
migration

Figure 2.7: **Models of RASSF1A contribution to MT functions and Golgi organization**

(A) Model of RASSF1A functions in interphase cells. (B) Model of the role of RASSF1A in directional cell migration.

Supplementary Materials

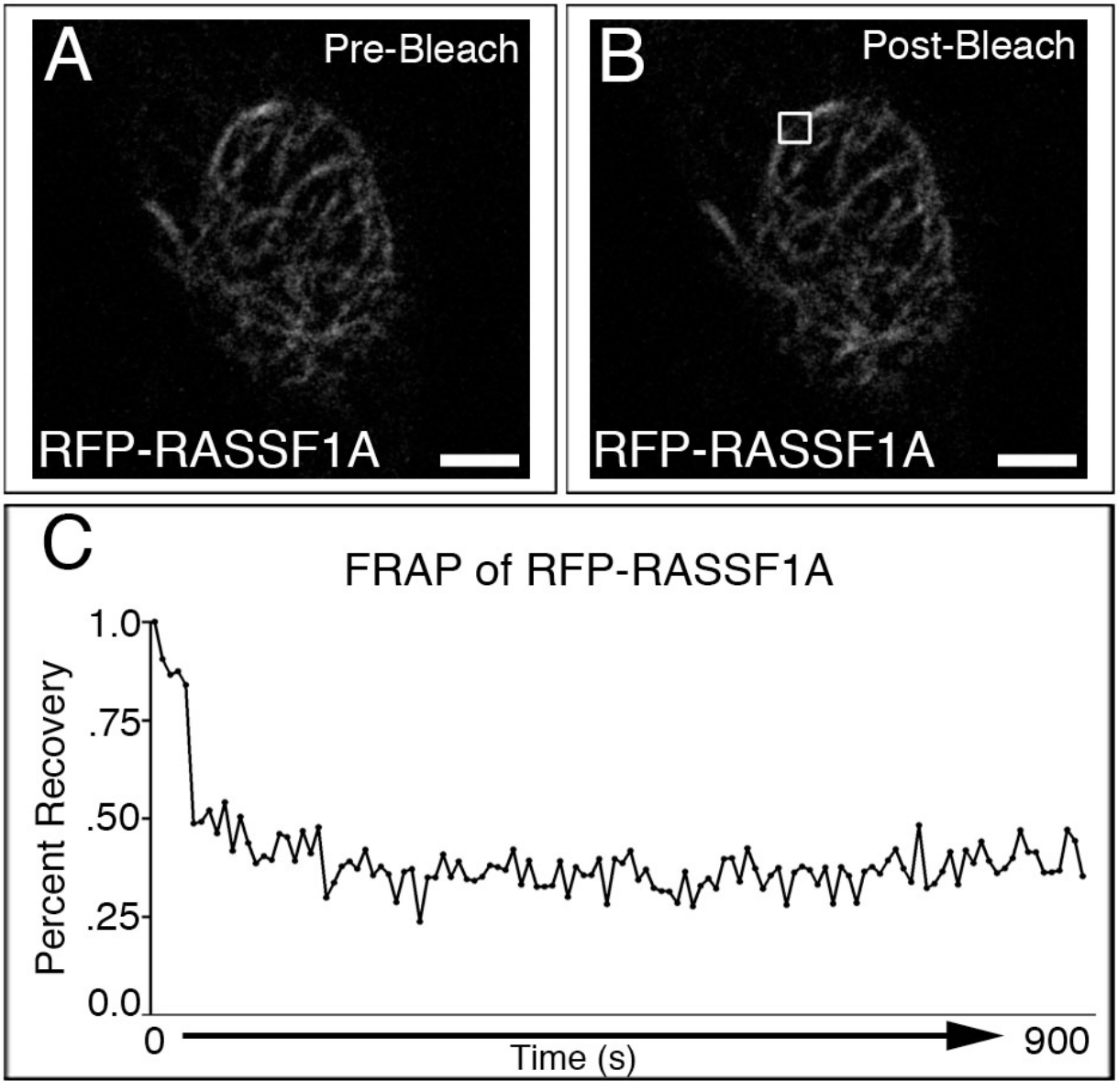

Figure 2.S1: RASSF1A is non-dynamic on MTs, related to Figure 2.4.

(A-B) HeLa GFP-Tubulin expressing cell transfected with RFP-RASSF1A pre- and post-bleach. White box indicates FRAP region. Bar, 5μm. (C) FRAP analysis of indicated region in *B* reveals that RFP-RASSF1A does not recover on MTs (spinning disk confocal,30s/frames.

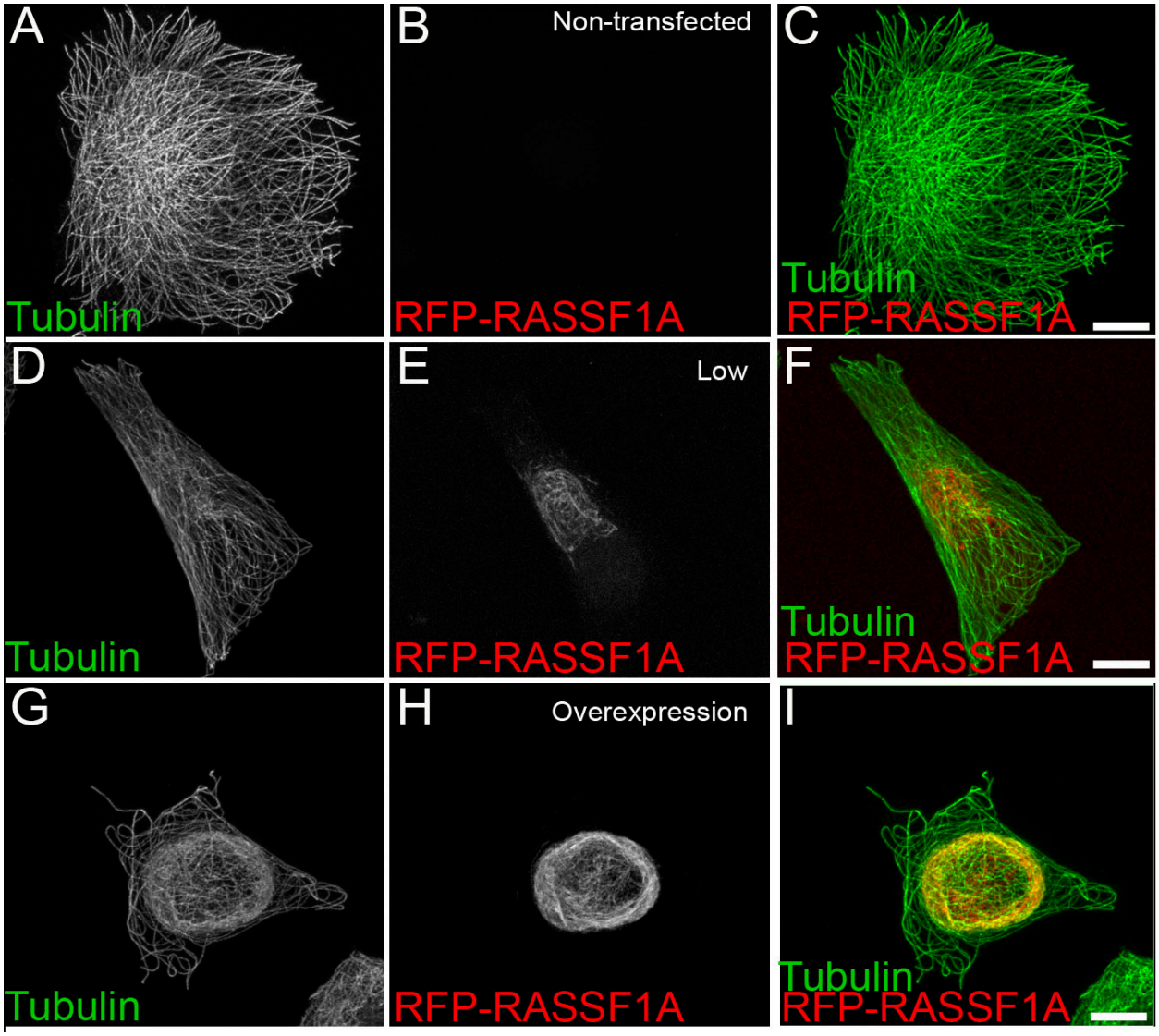
A
Tubulin
B
Non-transfected
RFP-RASSF1A
C
Tubulin
RFP-RASSF1A
D
Tubulin
E
Low
RFP-RASSF1A
F
Tubulin
RFP-RASSF1A
G
Tubulin
H
Overexpression
RFP-RASSF1A
I
Tubulin
RFP-RASSF1A

Figure 2.S2: RASSF1A expression alters MT network configuration, related to Figure 2.4.

(A-C) MCF-7 cell fixed and stained for Tubulin (green). Immunostaining. Cells exhibit a radial MT network configuration. (D-F) MCF-7 cell expressing low-levels of RFP-RASSF1A fixed and stained for Tubulin (green). Immunostaining. MT network organization is altered so that cells exhibit a more polarized morphology. (G-I) MCF-7 cell overexpressing RFP-RASSF1A fixed and stained for Tubulin (green). Immunostaining. MT network is highly bundled as compared with *C* and *F*. Bar, 5μm.

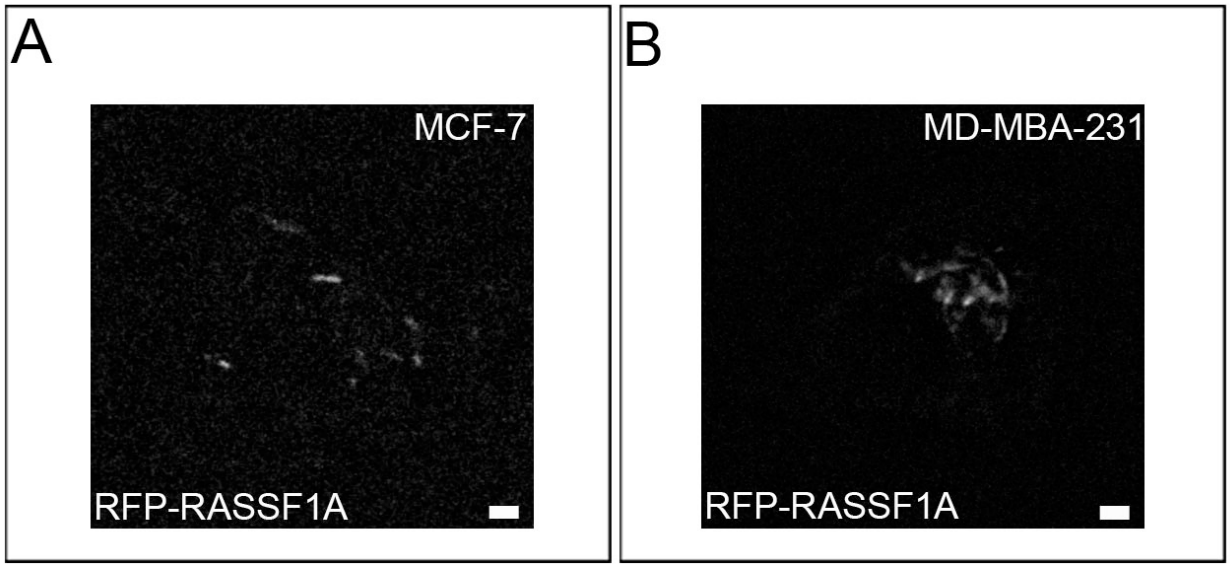
A
MCF-7
RFP-RASSF1A
B
MD-MBA-231
RFP-RASSF1A

Figure 2.S3: RFP-RASSF1A expression in MCF-7 and MD-MBA-231 cells, related to Fig 2.6.

(A-B) Representative images of RFP-RASSF1A cell transfection in MCF-7 and MD-MBA-231 used for protrusion circularity and directional persistence analysis in Figure 2.6, N and U. Bar, 10 μm.

Methods

Cells

Immortalized human retinal pigment epithelial cells, hTert-RPE1 (Clontech), were maintained in DMEM/F12 with 10% fetal bovine serum (FBS). H1792 human tumor cell [24] lines were grown in RPMI with 10% fetal calf serum. MCF-7 breast cancer cells (American Type Culture Collection, Manassas, VA) and HeLa GFP-Tubulin (a kind gift of Paul Chang, MIT) were grown in DMEM with 10% fetal bovine serum. Cells were grown in 5% CO_2 at 37°C. Cells were plated on fibronectin-coated glass coverslips 24 hours before experiments. In all live cell experiments, cells were maintained on the microscope stage at 37°C under mineral oil for media equilibrium maintenance.

Treatments

For MT depolymerization during live-cell imaging, cells were initially imaged in media lacking nocodazole (Sigma, St. Louis, MO). In the subsequent frames, the media was aspirated off and replaced with cell culture media containing nocodazole (2.5μg/ml) while imaging.

shRNA, siRNA and Expression Constructs

RASSF1A shRNA has previously been described in [24]. Single or a combination of single Stealth siRNA oligos against RASSF1A (HSS174151, HSS117377; Life Technologies, Invitrogen, Darmstadt, Germany) were transfected into RPE1 cells using

Lipofectamine RNAiMax (Invitrogen, Carlsbad, CA) according to the manufacturer's protocol. RASSF1HSS174151 siRNA targeted sequence: 5'-GGGACGCCUUCAGCAUGCCUGAACU-3'; RASSFHSS117377 siRNA targeted sequence: 5'-ACGCACAAGGGCACGUGAAGUCAUU-3'. Experiments were conducted 72 hours post-transfection as at this time minimal protein levels were detected. Non-targeting siRNA (Dharmacon, Thermo Scientific, Pittsburgh, PA) was used for controls. GFP-RASSF1A and RFP-RASSF1A have been described previously in [12] and [2], respectively. mCherry-EB3 (gift from J.V. Small, Vienna, Austria), EGFP-EB3 (gift from A. Akhmanova, Utrecht, The Netherlands) and 3x-GFP-EMTB (gift from J.C. Bulinski, New York, NY) were used for MT plus tip and MT visualization. RPE1 and MCF-7 cells were transfected with Fugene6 (Roche, Indianapolis, IN) according to manufacturer's protocols.

Antibodies and Immunofluorescence Details

For Golgi identification, mouse monoclonal antibody against GM130 (1:300; BD Transduction Laboratories, San Jose, CA) was used. MTs were stained with anti-α-tubulin rabbit polyclonal antibody (1:1000; Abcam, Cambridge, MA). For detyrosinated tubulin detection, a rabbit polyclonal antibody was used (1:500; Millipore, Billerica, MA). For MT and Golgi staining, cells were fixed (15' at room temp.) in 4% paraformaldehyde, 0.025% Glutaraldehyde, 0.3% Triton in cytoskeleton buffer (10 mM MES, 150 mM NaCL, 5 mM EGTA, 5 mM glucose, and 5 mM $MgCL_2$, pH 6.1). Alexa488-conjugated highly cross-absorbed goat anti-mouse IgG antibodies and Alexa488-conjugated goat

anti-rabbit IgG antibodies (1:500; Molecular Probes, Invitrogen, Eugene, OR) were used as secondary antibodies.

Confocal and live cell imaging

Leica TCS SP5 confocal laser scanning microscope with an HCX PL APO 100x oil lens NA 1.47 was used for taking confocal stacks of fixed cells and photo-bleaching of living cells.

TIRFM live-cell videos were acquired on a Nikon TE2000E microscope with Nikon TIRF2 System using a TIRFM 100x 1.49 NA oil lens, and Cascade 512B camera (Photometrics) and IPLab software (Scanalytics).

Live cells plated on MatTek glass bottom dishes were maintained at 37°C by heated stage (Warner Instruments). Single plane confocal video sequences were taken were taken by Yokogawa QLC-100/CSU-10 spinning-disk head (Visitec assembled by Vashaw) attached to Nikon TE2000E microscope using CFI PLAN APO VC 100X OIL lens, NA 1.4 with 1.5× intermediate magnification and back-illuminated EM-CCD camera Cascade 512B (Photometrics) driven by IPLab software (Scanalytics). 75 mW 488/568 Krypton-Argon laser (Melles Griot) with AOTF was used for 2-color excitation. Custom double dichroic mirror and filters (Chroma) in a filter wheel (Ludl) were used in the emission light path.

Western blot analysis

Western blotting was performed with the Protein Electrophoresis and Western Blotting System (Bio-Rad, Hercules, CA). For western blotting, a mouse polyclonal antibody against actin (1:1000; pan-Ab-5; Thermo Scientific, Pittsburgh, PA) and a mouse anti-human antibody against RASSF1A (1:500; EBioscience, San Diego, CA), were used. Nitrocellulose membrane was incubated with primary and then secondary antibody (LI-COR Bioscience, IRDye™ 800 and 700, Lincoln, NE) diluted in Odyssey Blocking Buffer with 0.2% Tween-20 to lower background. Odyssey Infrared Imaging System (LI-COR Bioscience, Lincoln, NE) was used for membrane scanning.

FRAP

FRAP was performed using Leica TCS SP5 confocal laser scanning microscope. ROI were introduced in cells expressing GFP-Tubulin and RFP-RASSF1A within RFP-RASSF1A segments. Photo-bleaching of said ROIs was carried out with 100 percent laser power of the 561 laser. Cells were then imaged for 15 minutes with 30-second intervals to monitor RFP-RASSF1A recovery.

Quantitative analyses:

MT Dynamics Parameters

To analyze MT dynamic parameters in NT control cells and RASSF1A-depleted cells, 5 min single channel TIRFM sequences (3 sec/frame) of cells expressing 3x-GFP-EMTB were used. Individual MTs were manually tracked using the MTrackJ plugin of ImageJ by following movements of the MT tip as visualized by 3x-GFP-EMTB

expression. Cells expressing low levels of 3x-GFP-EMTB were used to avoid analysis of cells with dampened MT dynamics. 20 MTs per condition (NT control or RASSF1A-depleted) were analyzed. Average number of events (rescue, catastrophe, pause and pause duration) were manually calculated per MT; This was then used to calculate the frequency (rescue and catastrophe) per MT/min. Average MT growth and shrinkage rate was calculated from instantaneous velocity measurements obtained from the MTrackJ plugin of ImageJ.

Distance Dispersal

Distance dispersal analysis was first performed with ImageJ. Golgi particles were subjected to thresholding and X, Y coordinates obtained using the Analyze Particles function of ImageJ. X, Y coordinates were then analyzed using a custom program written in MATLAB to calculate average distance between all particles.

Golgi Fragmentation

Golgi fragmentation analysis was performed with the Analyze Particles function of ImageJ. Golgi particles were subjected to thresholding and the number of particles was automatically calculated.

Fluorescence Intensity

Intensity in cells expressing various levels of RFP-RASSF1A was measured using ImageJ software. Cells of interest were outlined with a selection tool and measurements were set (Area, integrated density, and mean gray value). Three background

measurements were taken. To correct for background, the following formula was used: Corrected Total Cell Fluorescence = Integrated Density – (Area x Mean Fluorescence of Background Readings). Similar methods were used to determine fluorescence intensity of RFP-RASSF1A associated MTs and single, non-associated MTs.

Bundling and unbundling

Bundling analysis of non-RASSF1A-associated MTs was restricted to 1.5μm^2 ROIs (similar to the size of RASSF1A segments). The total number of ROIs analyzed was equal to the total number of RASSF1A segments in the cell. Bundling and unbundling events were quantified as those lasting two frames (10s) or more. Events per ROI were divided by the total number of MTs within the ROI to determine the "per MT" contribution to bundling (or unbundling). RASSF1A-associated MTs were quantified per RASSF1A fragment.

Cell Polarity

To analyze cell polarity, 6-hour DIC sequences (180s/frame) of cells depleted (RPE1) or expressing (MCF-7 and MD-MBA-231) RASSF1A were used. Cell polarity was analyzed by assessing the direction of cell protrusions formed throughout the time sequence. The initial area of the cell (Frame 1) was subtracted from the combined area taken by all protrusions in subsequent frames. The circularity of the resulting shape was quantified by ImageJ Circularity analysis. In this analysis, if protrusions were formed equally around the cell perimeter (lack of polarity), the overlaid protrusion area formed a

donut shape (circularity equals one). If protrusions form only at one side of a cell (high polarity), the overlaid area is significantly asymmetric (circularity approaches zero).

Statistical Analysis

Statistical significance was determined by Students t-test (two-tailed, unpaired).

Acknowledgements

The authors thank Ashley Grimaldi for providing technical and proofreading expertise. This work was supported by the NIH Integrated Biological Systems Training in Oncology (IBSTO) training grant (5T32CA119925-03) to C.A., American Heart Predoctoral Fellowship 12PRE12040218 (to C.A), NIH grant R01-GM078373 (to I.K.), and American Heart Association Grant-in-Aid 13GRNT16980096 (to I.K.).

CHAPTER III

Microtubule and Actin interplay drive intracellular c-Src trafficking in VSMCs

Abstract

The proto-oncogene c-Src is a non-receptor tyrosine kinase that is involved in a variety of signaling processes that can regulate cell migration, adhesion, cell division, and survival in both normal and cancer cells. c-Src is rarely mutated during cancer transformation, but instead exhibits elevated expression levels in a variety of cancers. Therefore, c-Src localization must be tightly regulated to prevent aberrant phosphorylation of downstream targets; however, the true mechanism of c-Src trafficking is unclear. Thus, we tested the hypothesis that regulation of c-Src trafficking requires cytoskeletal crosstalk between microtubules and actin, which is mediated by GEF-H1 and RhoB. Our results show that c-Src vesicles move bidirectionally along microtubules; however, microtubule depolymerization leads to faster, but less directional c-Src vesicle trafficking, in addition to increased actin comet formation at c-Src vesicle membranes. Moreover, microtubule depolymerization also increased RhoB activation. Furthermore, loss of GEF-H1 activity significantly impaired actin comet tail formation and RhoB activation. These results indicate that c-Src trafficking is tightly regulated process that requires the coordinated efforts of both major cytoskeletal elements for efficient delivery to the plasma membrane.

Introduction

c-Src is a non-receptor tyrosine kinase that has been implicated in pathways regulating angiogenesis, invasion and metastasis, cell migration, endocytosis, and many others. When inactive, c-Src is associated with the plasma membrane through an N-terminal fatty acid moiety. However, during activation, c-Src is released so that it can translocate to interact with its effectors (Bjorge *et al.*, 2000). As such, when c-Src becomes deregulated, the effects can manifest in the processes that c-Src regulates, leading to several hallmarks of cancer(Hanahan and Weinberg, 2000; Yeatman, 2004). Frequently, increased c-Src expression and activity is associated with many malignancies, strongly suggesting a role for c-Src in oncogenesis (Alvarez *et al.*, 2006); However, despite the increasing evidence for the role of c-Src in cancer transformation, c-Src alone is incapable of transforming human cells *in vitro*, and very few transforming mutations have been identified in human cancers(Shalloway *et al.*, 1984; Irby *et al.*, 1999). Furthermore, during atherosclerotic plaque formation, vascular smooth muscle cells (VSMCs) assume a synthetic phenotype, whereby they become highly migratory and invasive. This process is mediated by the formation of invasive structures, podosomes, which are dependent upon c-Src localization to the plasma membrane. Therefore, since c-Src is involved in so many processes, the subcellular localization of c-Src is critical to its function (Biscardi *et al.*, 1999).

Currently, the mechanism by which c-Src is positioned within the cell is under debate. Whether the local positioning of c-Src within the cell is a MT-dependent, actin-dependent, or some combinatorial mechanism has yet to be identified. Although evidence for the first two scenarios exists, they do not completely reconcile the

discrepancies found throughout the literature. Studies have indicated that inactive c-Src can be localized to the perinuclear region, colocalizing with endosomal and Golgi markers (Kaplan *et al.*, 1992), and upon activation, it can be subsequently targeted to the cell periphery (Timpson *et al.*, 2001). However, at present, the mechanism by which c-Src is localized in response to cellular cues is still quite not understood. In neuronal growth cones, trafficking of endosomal c-Src was identified as a MT-dependent process that allowed for bidirectional trafficking along the MT network (Wu *et al.*, 2008). Depolymerization of MTs lead to an accumulation of plasma membrane-associated c-Src, indicating a dependence on MTs, and not other cytoskeletal elements, for c-Src vesicle recycling in growth cones. Conversely, c-Src endosomal trafficking has also been identified as an actin-dependent process. c-Src was found to mainly associate with RhoB-containing cytoplasmic endosomes which also contained actin nucleating machinery, specifically Scar1/WAVE1 and mDia2 (Sandilands *et al.*, 2004).

Here, we applied high-resolution confocal microscopy and biochemical techniques to determine the mechanism of c-Src trafficking, as well as the activation status of the molecular players involved. We determined that c-Src is trafficked bidirectionally along MTs; however, MT depolymerization does not inhibit c-Src vesicle movement, but instead, leads to faster, less directional movement. Furthermore, MT depolymerization resulted in increased actin comet tail formation at c-Src vesicle membranes. Regulation of these actin comet tails was found to be dependent on MT-associated GEF, GEF-H1. Inhibition of GEF-H1 activity or constitutive activation resulted in decreased actin comet tails or actin comet tail formation similar to nocodazole-treated controls, respectively. Additionally, we also found that RhoB was

also trafficked bidirectionally along MTs and associated with a subset of c-Src vesicles. Moreover, MT depolymerization also lead to increased RhoB activation in these cells. This study provides the first evidence of the coordinated efforts of the MT and actin cytoskeleton in correctly trafficking c-Src from the perinuclear region to the cell periphery.

Results

c-Src traffics bidirectionally on MTs

The goal of this study was to investigate the molecular mechanism by which c-Src is trafficked and whether this trafficking required the cooperative action of both the MT and actin cytoskeleton. To address this, we utilized a cell culture system including Retinal Pigment Epithelial cells (RPE1) and rat aortic vascular smooth muscle cells (VSMCs). Because previous reports have shown that c-Src can be trafficked independently by both MTs (MTs) (Wu *et al.*, 2008), we first determined whether this mechanism existed in our system. We found that GFP-Src on endosomal membranes was trafficked bidirectionally along MTs (Figure 3.1 A-A’’’’’) from the cell center and cell periphery. Depolymerization of MTs by the MT-depolymerizing drug, nocodazole, did not inhibit GFP-Src trafficking, but instead disrupted the trajectory of GFP-Src vesicles, restricting them spatially within the cytoplasm (Figure 3.1 B, C). Analysis of GFP-Src vesicle velocity under control and nocodazole-treated conditions revealed that upon MT depolymerization, GFP-Src vesicle velocity significantly increased (Figure 3.1 D). Additionally, analysis of vesicle directionality under these conditions reveals that vesicle movement becomes highly randomized as compared to control (Figure 3.1 E). We hypothesize that the continued movement of c-Src vesicles upon MT depolymerization may represent a secondary, but less efficient mechanism by which c-Src may be trafficked or may represent a part of a larger mechanism of c-Src trafficking whereby MTs provide long-range, directional trafficking and this secondary mechanism provides short-range delivery to the plasma membrane.

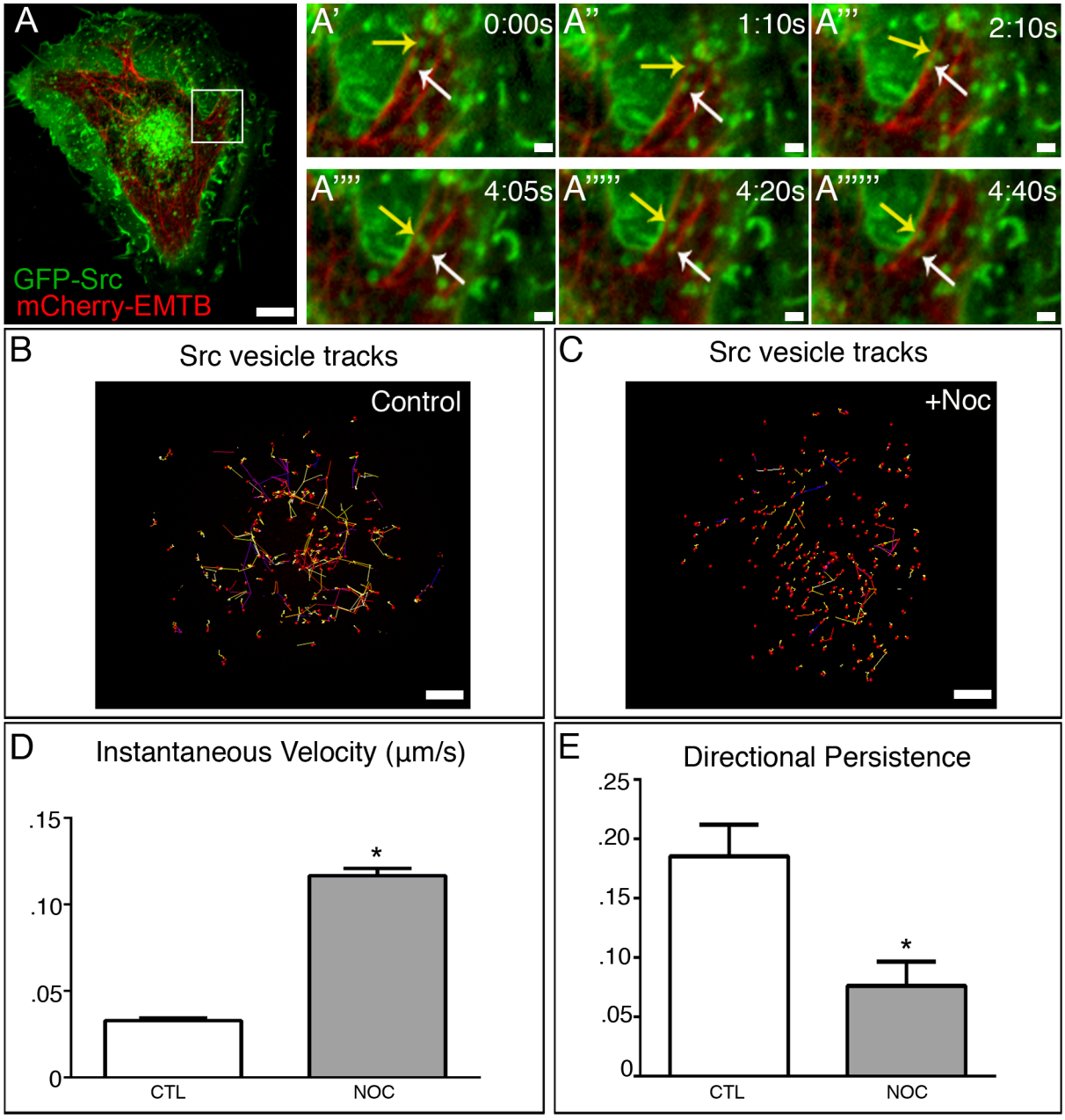
A
A'
0:00s
A''
1:10s
A'''
2:10s
A''''
4:05s
A'''''
4:20s
A''''''
4:40s
GFP-Src
mCherry-EMTB
B
Src vesicle tracks
Control
C
Src vesicle tracks
+Noc
D
Instantaneous Velocity (µm/s)
.15
.10
.05
0
*
CTL
NOC
E
Directional Persistence
.25
.20
.15
.10
.05
0
*
CTL
NOC

Figure 3.1: c-Src exhibits bimodal trafficking

(A) Detection of GFP-Src (green) and 3x-mCherry-EMTB (red) in time-lapse confocal movie of an A7r5 cell. Area in box is enlarged to the right. Bar, 5μm. (A'-A''''') Imaging sequence illustrates that GFP-Src is trafficked bidirectionally along MTs in *A.* Bar, 2μm (B) GFP-Src vesicles exhibit long, directional movement in time-lapse confocal movie of an A7r5 control (5s/frames). Representative tracks. Bar, 5μm. (C) GFP-Src vesicles exhibit short, randomized movement in time-lapse confocal movie of an A7r5 control (5s/frames). Representative tracks. Bar 5μm. (D) GFP-Src vesicles exhibit increased velocity in response to MT depolymerization. (D) GFP-Src vesicles show reduced directional persistence following nocodazole treatment.

MT depolymerization induces actin comet tail formation through regulating GEF-H1

Previous reports have demonstrated that c-Src trafficking may also be mediated through the action of actin nucleating machinery, particularly adaptor protein Scar1/Wave1 and actin filament regulatory protein, mdDia2 (Sandilands *et al.*, 2004). To determine whether actin polymerization was the driving force behind c-Src vesicular movement upon MT depolymerization, we applied live-cell confocal microscopy imaging of cells co-expressing GFP-Src and RFP-cortactin, a marker of polymerizing actin. Additionally, we coupled this with immunofluorescence techniques to provide an overall idea of the magnitude of actin polymerization occurring. In both cases, we found that upon MT depolymerization, the number of actin comets formed significantly increased (Figure 3.2 A-C). Not surprisingly, we also found that association of cortactin puncta with c-Src vesicles was also increased upon MT depolymerization (Figure 3.2 D-F)

These data suggest that MT regulation of some factor is perturbed upon MT depolymerization, allowing said factor to interact with actin nucleating machinery. As GEF-H1, a Rho GEFs regulated by MT binding (Krendel *et al.*, 2002), has been implicated in being a mediator of cytoskeletal crosstalk (Birkenfeld *et al.*, 2007; Chang *et al.*, 2008), we examined whether it was involved in potentiating the formation of actin comet tails upon MT depolymerization. Utilizing cortactin as a marker of actin comet tail formation, we tested for formation by immunostaining in VSMCs transiently expressing various GFP-GEF-H1 constructs. GFP-GEF-H1-wild type (GEF-WT) expressing cells exhibited few actin comet tails prior to MT depolymerization, but this significantly

increased after treatment with nocodazole (Figure 3.2 G, K and J). In cells expressing GFP-GEF-H1-dominant negative (GEF-DN), actin comet tail formation was inhibited both in control and nocodazole treated cells (Figure 3.2 H, L, and J), further implicating GEF-H1 in mediating cytoskeletal crosstalk in our cells. Furthermore, cells expressing GFP-GEF-H1-constitutively active (GEF-CA) exhibited increased actin comet tail formation in the presence and absence of MTs, similar to levels seen in nocodazole-treated control (Figure 3.2 I, M, and J). Thus, actin comet tail formation at c-Src vesicle membranes, through the action of GEF-H1, might serve as a secondary mechanism to increase the efficiency of c-Src trafficking.

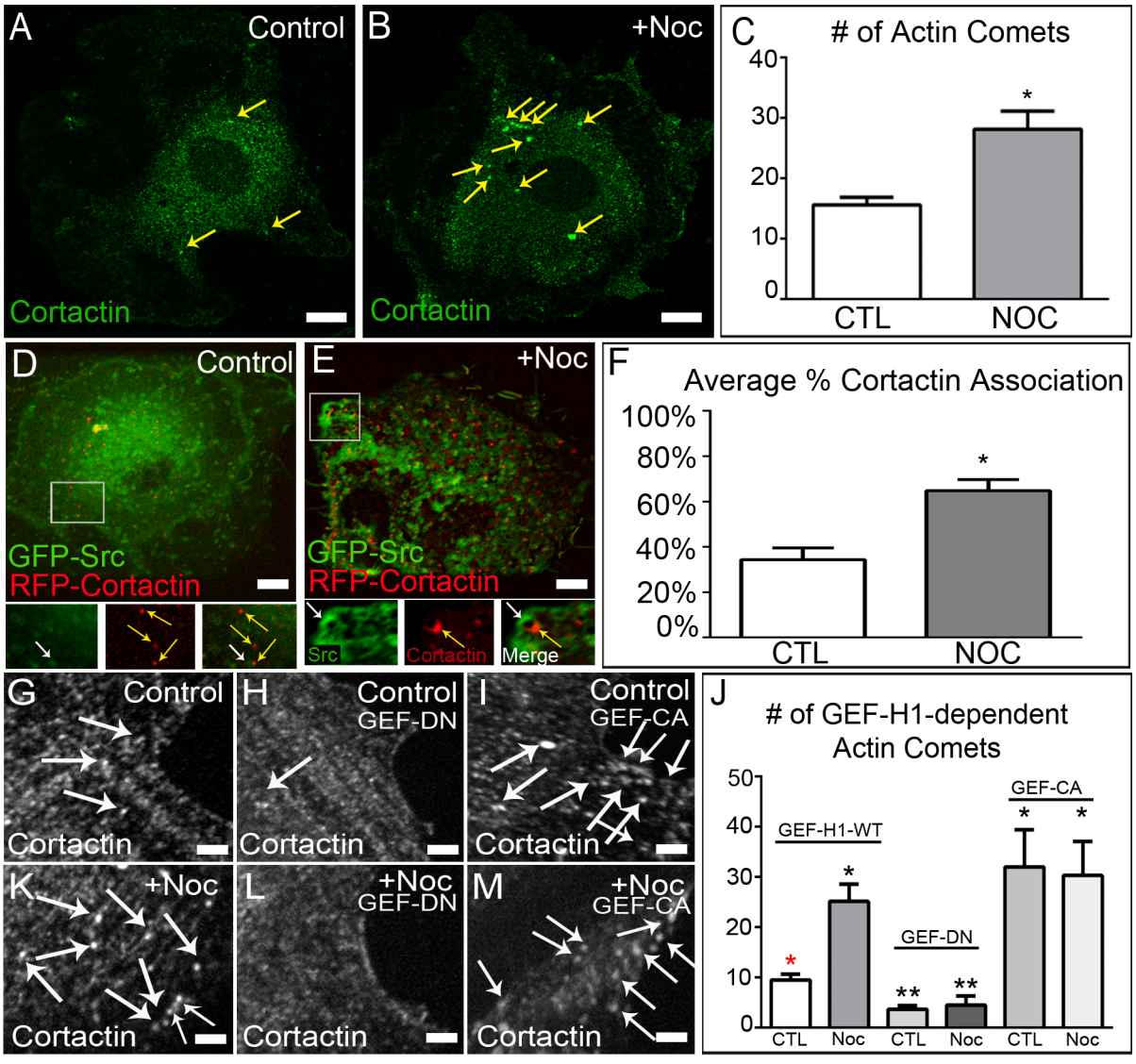
A
Control
Cortactin
B
+Noc
Cortactin
C
# of Actin Comets
40
30
20
10
0
*
CTL
NOC
D
Control
GFP-Src
RFP-Cortactin
E
+Noc
GFP-Src
RFP-Cortactin
Src
Cortactin
Merge
F
Average % Cortactin Association
100%
80%
60%
40%
20%
0%
*
CTL
NOC
G
Control
Cortactin
H
Control
GEF-DN
Cortactin
I
Control
GEF-CA
Cortactin
J
# of GEF-H1-dependent
Actin Comets
50
40
30
20
10
0
GEF-H1-WT
GEF-DN
GEF-CA
*
**
CTL
Noc
CTL
Noc
CTL
Noc
K
+Noc
Cortactin
L
+Noc
GEF-DN
Cortactin
M
+Noc
GEF-CA
Cortactin

Figure 3.2: GEF-H1 regulates formation of actin comet tails at c-Src vesicle membranes

(A-B) Control and nocodazole-treated A7r5 cells fixed and stained for cortactin (green). Immunostaining. Bar, 5μm. (C) Quantification of actin comet tail formation in control and nocodazole-treated cells reveals a two-fold increase upon MT depolymerization. Representative examples out of 30 cells/condition. Error bars indicate s.e.m. (D-E) Live-cell imaging of control and nocodazole-treated A7r5 cells expressing GFP-Src and RFP-Cortactin. Area in box is enlarged below. Bar 5μm. (F) Quantification reveals that MT depolymerization induces increased actin comet formation at c-Src vesicle membranes. (G and K) Z-section of A7r5 cells expressing wild-type GEF-H1 pre- and post-nocodazole fixed and immunostained for cortactin. Images illustrate an increase in cortactin puncta (white arrows) following MT depolymerization Bar, 5μm. (H and L) Z-section of A7r5 cells expressing dominant-negative GEF-H1 pre- and post-nocodazole demonstrates the role of GEF-H1 in forming actin comets. Bar, 5μm. (I and M) Z-section of A7r5 cells expressing constitutively active GEF-H1 pre- and post-nocodazole show high number of actin comets in the presence or absence of MTs. Bar, 5μm. (J) Quantification of actin comet tail formation after expression of various GEF-H1 constructs. Representative examples out of 30 cells/condition. Error bars indicate s.e.m.

RhoB associates with c-Src vesicle membranes

It has previously been identified that actin-dependent trafficking of c-Src vesicles relied on RhoB localization at the vesicle membrane (Sandilands *et al.*, 2004). Moreover, actin nucleating machinery, Scar1/Wave1 and mDia2, were also shown to be required for efficient trafficking of c-Src to the cell periphery(Sandilands *et al.*, 2004). However, as c-Src was shown to traffic by MTs (Wu *et al.*, 2008), we tested whether RhoB-associated vesicles could also be trafficked in a similar manner. We utilized live-cell confocal imaging of cells expressing GFP-RhoB and 3x-mCherry-EMTB and tracked vesicle movement. Our data shows that GFP-RhoB vesicles could traffic bidirectionally along MTs (Figure 3.3 A-A’’’) in a manner similar to c-Src vesicles. We hypothesize that the localization of RhoB vesicles on MTs is important for association with c-Src vesicles and may facilitate actin polymerization at c-Src vesicle membranes. To address whether c-Src and RhoB localized within the same vesicle, cells expressing GFP-RhoB and mCherry-Src were imaged by spinning-disk confocal microscopy. Our data shows that GFP-RhoB colocalized with a subset of mCherry-Src vesicles (Figure 3.3 B-B’’’ and C) particularly at one side of the vesicle membrane. Positioning of RhoB at c-Src vesicles membranes may serve as a mechanism by which actin polymerization can be precisely localized and quickly initiated at c-Src vesicles. Localized positioning of RhoB at one site on c-Src vesicle membranes may facilitate asymmetric actin polymerization. Therefore, this localization potentially increases the efficiency of c-Src trafficking by sequestering components necessary to provide force at c-Src vesicle membranes.

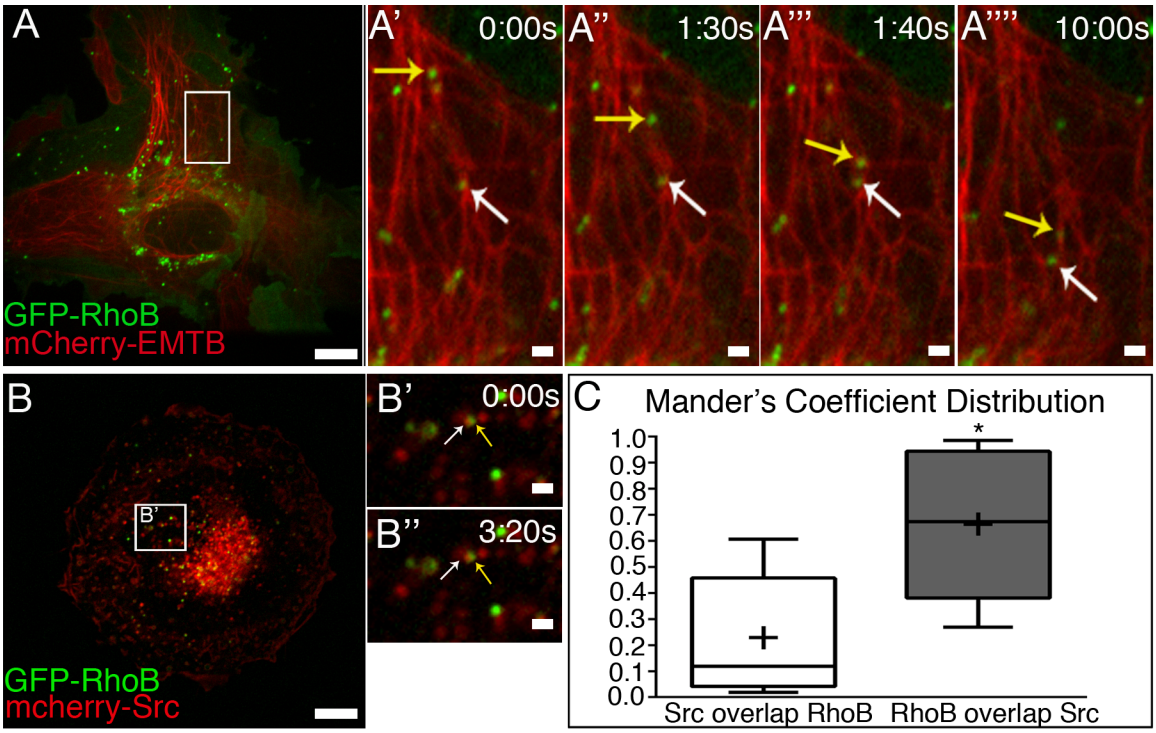
A
A'
0:00s
A''
1:30s
A'''
1:40s
A''''
10:00s
GFP-RhoB
mCherry-EMTB
B
B'
GFP-RhoB
mcherry-Src
B'
0:00s
B''
3:20s
C
Mander's Coefficient Distribution
1.0
0.9
0.8
0.7
0.6
0.5
0.4
0.3
0.2
0.1
0.0
*
Src overlap RhoB
RhoB overlap Src

Figure 3.3: RhoB is trafficked along MTs and associates with c-Src vesicles

(A) A7r5 cells expressing GFP-RhoB (green) and 3X-mCherry-EMTB (red). Area in box is enlarged to the right. Spinning disk confocal. Bar, 5μm. (A' – A'''') Time-lapse confocal microscopy reveals vesicles GFP-RhoB move along MTs (yellow and white arrows). Bar, 2μm. (B) A7r5 cell expressing GFP-RhoB (green) and mCherry-Src (red). Area in box is enlarged to the right. Spinning disk confocal. Bar, 5μm. (B' – B'') Time-lapse confocal microscopy shows that GFP-RhoB (yellow arrows) can associate with a subset of mcherry-Src vesicles (white arrows). (C) Mander's coefficient distribution reveals that the majority of GFP-RhoB vesicles are associated with mCherry-Src.

RhoB is activated by MT depolymerization

Prior reports have indicated that actin-dependent trafficking of c-Src vesicles relies on the activity of Rho GTPase, RhoB (Sandilands *et al.*, 2004). Additionally, it has been shown that Rho GEF, GEF-H1, can interact with an activate RhoB to elicit actin polymerization (Kamon *et al.*, 2006; Vega *et al.*, 2012). Because MT depolymerization clearly imparts a specialized trafficking ability of c-Src vesicles by actin comet tails, we next addressed their formation through activation of Rho GTPase, RhoB. We hypothesized that MT depolymerization can allow GEF-H1 to interact with and activate downstream effector RhoB for the formation of actin comet tails. To assess RhoB activation in the absence or presence of MT depolymerization, RBD-RhoB pulldowns were performed and immunoblotted for activated Rho. Analysis revealed that upon MT depolymerization RhoB exhibited a 15%-30% increase in their RhoB activity (Figure 3.4 A and B). Thus, RhoB activity can be modulated by the presence or absence of an intact MT network. This regulation of RhoB activity may be even more significant out at the cell periphery, as the ability of MTs to undergo dynamic instability could fine-tune the final step in delivery of c-Src vesicle to the plasma membrane through localized release of GEF-H1 and RhoB activation, thus initiating actin polymerization.

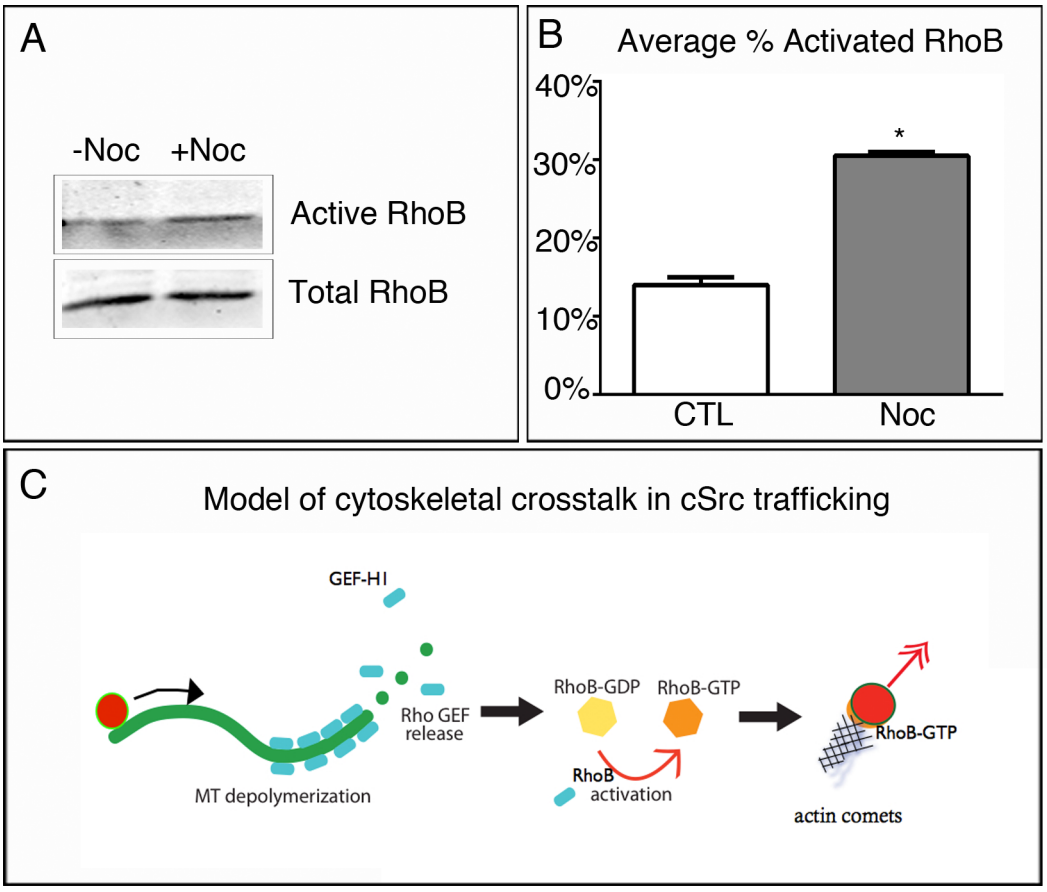
A
-Noc
+Noc
Active RhoB
Total RhoB
B
Average % Activated RhoB
40%
30%
20%
10%
0%
*
CTL
Noc
C
Model of cytoskeletal crosstalk in cSrc trafficking
GEF-H1
Rho GEF release
MT depolymerization
RhoB-GDP
RhoB-GTP
RhoB activation
RhoB-GTP
actin comets

Figure 3.4: RhoB is activated by MT depolymerization

(A) Western blot analysis of RhoB activation in response to MT depolymerization in control and nocodazole-treated RPE1 cells. (B) Quantification of average percent of RhoB activation from A reveals that RhoB activation is significantly higher following MT depolymerization. (C) Model of cytoskeletal crosstalk for c-Src delivery.

Discussion

In this study, we have sought to define a molecular pathway for trafficking of proto-oncogene, c-Src, in addition to resolving a longstanding debate on the involvement of the MT and actin cytoskeletons. We have found that c-Src can be trafficked bidirectionally along MTs; however, in the absence of MTs, actin comet tail formation at c-Src vesicle membranes could provide the necessary force to mediate c-Src vesicle movement. This bimodal mechanism of trafficking may represent two distinct mechanisms that have converged to increase the efficiency of c-Src vesicle trafficking. Alternatively, this may also represent one singular, combinatorial mechanism. In the latter, actin polymerization at c-Src vesicular membranes would provide the force necessary to propel vesicles along MT tracks. Then, upon MT depolymerization, further facilitate the process of c-Src trafficking in a faster, less directional manner. Limited imaging capabilities have hindered the ability to test this hypothesis, however, it seems high unlikely as we know that this process of actin comet tails formation seems to be greatly influenced by the activity of GEF-H1, which would be inactive through binding to intact MTs near the perinuclear regions where c-Src has been found to accumulate in an inactive state (Radziwill *et al.*, 2007; Walker *et al.*, 2007). Conversely, it may also be possible that some yet unidentified Rho GEF could potentiate this combinatorial process. Though the idea of cytoskeletal crosstalk is a well-studied phenomenon, particularly in the context of identifying molecules that mediate this crosstalk; the functional consequence of lack of one or both of these cytoskeletal elements on vesicular trafficking or the processes they regulate has not been as well defined.

Furthermore, our data suggests that the switch from MT to actin-based motility is mediated by the activity of GEF-H1, and that inhibition of GEF-H1 activity severely impairs the ability of actin comet tail formation. This evidence places GEF-H1 within the molecular pathway that defines the mechanism of c-Src trafficking. Though evidence for GEF-H1 activating other Rho GTPases exists, this data suggests that GEF-H1 has the ability to differentially regulate these Rho GTPases within the local environment. The regulation of c-Src trafficking has a variety of implications, particularly in disease progression. Thus, this regulation by GEF-H1 may be significant for formation of actin comets at c-Src vesicle membranes within the cell periphery, as c-Src at the periphery must be correctly localized and positioned at the plasma membrane for the formation of invasive structures, podosomes, that aid in VSMC migration during atherosclerotic plaque development (Zahradka *et al.*, 2009).

At the same time, we show that RhoB at vesicle membranes can traffic bidirectionally along the MT network, in addition to associating c-Src vesicle membranes. We hypothesize that the localization of RhoB at c-Src defines the sites of preferred actin comet tail formation on c-Src vesicle membranes. In this scenario, RhoB puncta at vesicle membranes would facilitate asymmetric actin polymerization on the c-Src vesicle membrane during MT depolymerization, providing the force necessary to propel c-Src vesicles at the cell periphery. Ultimately, we can infer that a disruption mislocalization of RhoB from c-Src vesicle membranes would specifically interfere with vesicular trafficking of c-Src vesicles, and the long-term effects would manifest in diminished or loss of c-Src signaling in cells.

Additionally, we show that RhoB is activated upon MT depolymerization. We hypothesize that this activation of RhoB is mediated by GEF-H1 and occurs at c-Src vesicle membranes to facilitate actin polymerization. With this idea, inhibition of GEF-H1 activity would lead to loss of actin comet tail formation and cessation of c-Src vesicle movement following MT depolymerization. Moreover, lack of the RhoB activation may inhibit trafficking and fusion of c-Src vesicles at the plasma membrane. Ultimately, we can infer that perturbations to RhoB activation may result in significant alterations in c-Src activity both in the cytoplasm and at the plasma membrane.

Collectively, our results have highlighted a mechanism by which c-Src can be properly trafficked and positioned (Figure 3.4 C). This mechanism probably contributes to the regulation of c-Src to prevent aberrant signaling. In particular, precise spatial regulation of c-Src is necessary to prevent aberrant cell migration through the formation of invasive structures, podosomes, structures that rely on c-Src for their establishment and maintenance. Our finding allows us to hypothesize an established dependence of c-Src localization on GEF-H1 and RhoB activation, which arises from the crosstalk between the MT and actin cytoskeleton.

Methods

Cells

Immortalized human retinal pigment epithelial cells, hTert-RPE1 (Clontech), were maintained in DMEM/F12 with 10% fetal bovine serum (FBS) and 5% L-glutamine. Rat aortic vascular smooth muscle cells (A7r5) were grown in DMEM with 10% fetal calf serum and 5% L-glutamine. Cells were plated on fibronectin-coated glass coverslips 24 hours before experiments. In all live cell experiments, cells were maintained on the microscope stage at 37°C under mineral oil for media equilibrium maintenance.

Treatments

For MT depolymerization, cells were incubated in 2.5μg/ml nocodazole (Sigma, St. Louis, MO) 2 hours prior to imaging. For RBD-RhoB pulldowns, cells were incubated in nocodazole for 30 minutes prior to cell lysis and incubation.

Expression Constructs

GFP-Src has previously been described (Sandilands *et al.*, 2004) was provided by Dr. Giulio Superti-Furga (EMBL, Heidelberg, Germany). GFP-GEF-H1 and GEF-GEF-H1 1-573 (gifts from Gary Bokoch, La Jolla, CA). GEF-DN and GFP-RhoB were purchased from addgene (Cambridge, MA). 3x-mCherry-EMTB (gift from William Bement, Madison, WI) was used for MT visualization. RFP-cortactin was provided by Marko Kaksonen (U.C. Berkeley) and used to visualize actin comet tail formation. RPE1

and A7r5 cells were transfected with Fugene6 (Roche, Indianapolis, IN) according to manufacturer's protocols.

Antibodies and Immunofluorescence Details

For actin comet tail identification, mouse monoclonal antibody against cortactin (1:1000; Upstate, Lake Placid, NY) was used. Cells were fixed (5' at 20°.) in 100% methanol. Alexa488-conjugated highly cross-absorbed goat anti-mouse IgG antibody (1:500; Molecular Probes, Invitrogen, Eugene, OR) was used as secondary antibodies.

Confocal and live cell imaging

Leica TCS SP5 confocal laser scanning microscope with an HCX PL APO 100x oil lens NA 1.47 was used for taking confocal stacks of fixed cells.

Live cells plated on MatTek glass bottom dishes were maintained at 37°C by heated stage (Warner Instruments). Single plane confocal video sequences were taken were taken by Yokogawa QLC-100/CSU-10 spinning-disk head (Visitec assembled by Vashaw) attached to Nikon TE2000E microscope using CFI PLAN APO VC 100X OIL lens, NA 1.4 with 1.5× intermediate magnification and back-illuminated EM-CCD camera Cascade 512B (Photometrics) driven by IPLab software (Scanalytics). 75 mW 488/568 Krypton-Argon laser (Melles Griot) with AOTF was used for 2-color excitation. Custom double dichroic mirror and filters (Chroma) in a filter wheel (Ludl) were used in the emission light path.

Western blot analysis

Western blotting was performed with the Protein Electrophoresis and Western Blotting System (Bio-Rad, Hercules, CA). For western blotting, a rabbit polyclonal antibody against RhoB (1:500; Cell Biolabs, San Diego, CA) was used. Nitrocellulose membrane was incubated with primary and then secondary antibody (LI-COR Bioscience, IRDye™ 800, Lincoln, NE) diluted in Odyssey Blocking Buffer with 0.2% Tween-20 to lower background. Odyssey Infrared Imaging System (LI-COR Bioscience, Lincoln, NE) was used for membrane scanning.

RhoB Activation

Cells were stimulated for 30 minutes, washed with ice-cold PBS and lysed in in buffer containing 125mM Hepes, pH 7.5, 750 mM NaCL, 5% NP-40, 50mM $MgCl_2$, 5mM EDTA, and 10% glycerol, supplemented with protease inhibitors. Lysates were cleared by centrifugation (14,000 rpm, 10min). A sample of supernatant was removed and lysates incubated with RBD beads for 1 hour at 4°C. Beads were washed three times with lysis buffer and protein cleaved by addition of 2x sample buffer. Samples were boiled and analyzed by Western blotting.

Quantitative analyses:

c-Src vesicle trafficking analysis

To analyze vesicle directionality and velocity in control cells and nocodazole-treated cells, 5 min one-channel confocal sequences (5 sec/frame) of cells expressing

GFP-Src were used. Individual vesicles were manually tracked using the MTrackJ plugin of ImageJ by following movements of the vesicles as visualized by GFP-Src expression. 50 vesicles per condition (control or nocodazole-treated) were analyzed. Average velocity was calculated from instantaneous velocity measurements obtained from the MTrackJ plugin of ImageJ. Directional persistence of vesicles was quantified as final distance of vesicle relocation divided by total vesicle track length.

Cortactin quantification

Leica confocal z-sections were obtained of control and nocodazole-treated cells stained for cortactin. Maximum intensity z-projections of three central slices were used for thresholding of cortactin puncta. Number of cortactin puncta under each condition was automatically quantified by ImageJ analysis. Similar methods were used upon expression of various GEF-H1 constructs.

Cortactin association with c-Src vesicles

Cortactin association analysis of control and nocodazole-treated cells was restricted to 4μm^2 ROIs. Cortactin association was scored 2.5 minutes after initiation of image acquisition. Number of cortactin-associated c-Src vesicles was visually scored and divided by the total number of c-Src vesicles within an ROI to determine association percentage.

Mander's Coefficient Distribution

To determine the degree of overlap, the first frame of live-cell confocal imaging sequences in A7r5 cells was used. Images were subjected to thresholding in the JaCOP plugin of ImageJ and Mander's coefficient was automatically calculated for the degree of overlap of GFP-RhoB and mCherry-Src.

Statistical Analysis

Statistical significance was determined by Students t-test (two-tailed, unpaired).

Acknowledgements

This work was supported by the NIH Integrated Biological Systems Training in Oncology (IBSTO) training grant (5T32CA119925-03) to C.A., American Heart Predoctoral Fellowship 12PRE12040218 (to C.A), NIH grant R01-GM078373 (to I.K.), and American Heart Association Grant-in-Aid 13GRNT16980096 (to I.K.).

CHAPTER IV

Conclusions and Future Directions

Conclusions

The studies presented here contribute to a better understanding of the cell biological function of how RASSF1A impacts the processes of MT network organization and cell polarity and migration, in addition to its newly discovered role on impacting Golgi organization. These findings shed new light on the far-reaching consequences of MAP binding on the diverse processes mediated by microtubules. Biologically, this is important due to the fact that regulation of MT dynamics and reorganization, as well as Golgi organization, all contribute to proper cell migration, which is an essential process for embryonic development, wound healing, and cancer invasion and metastasis (Magdalena *et al.*, 2003; Harris and Peifer, 2007; Prager-Khoutorsky *et al.*, 2007). This study provides the first functional insight into the role of RASSF1A on interphase MTs and also identifies major functions of RASSF1A in Golgi organization and cell polarity. Additionally, we also provide mechanistic evidence of the bimodal transport of c-Src in vascular smooth muscle cells. While the currently hypothesized mechanisms of c-Src trafficking rely only one component of the cytoskeleton (MTs or actin), these findings resolve the long-standing debate about the true mechanism of c-Src trafficking. Moreover, this work highlights the cooperative nature of cytoskeletal crosstalk that cells employ to correctly position proteins. This positioning of c-Src is extremely important due to the fact that c-Src is critical for processes such as cell-cycle progression, cell

migration, and invasion (Sanjay *et al.*, 2001; Kim *et al.*, 2013; De Luca *et al.*, 2014). With this study, we provide insight into the regulatory mechanism underlying c-Src trafficking.

Chapter II addresses the cell biological functions of microtubule-associated protein, RASSF1A. Here, we describe the role that RASSF1A has on regulating MT dynamics and stability, in addition, to the role that RASSF1A plays in organizing the Golgi and in cell polarity. In terms of dynamics and stability, MT dynamic instability allows for rapid reorganization of the MT network in response to cellular cues. Lack of dynamicity can negatively impact processes such as cell migration and division. RASSF1A segmental localization to MTs not only provide local methods of stabilizing and protecting MTs from completely depolymerizing, but can also function as sites of rescue, which are necessary to alter the existing MT network. Interestingly, RASSF1A could also induce local bundling of MTs both at the Golgi and within the MT network to induce further stabilization of MTs. The localization of RASSF1A to the Golgi and stabilization of MTs is extremely important, as this can provide the necessary platform on which Golgi organization can occur and the stable MT tracks which allow for directed cell migration and trafficking. In examining cells that had lost RASSF1A expression, we can see that the Golgi has become completely dispersed and randomized throughout the cytoplasm, highlighting the role for stable MT subsets on which proper Golgi organization must occur. Additionally, we can see that re-expression of RASSF1A can reverse this dispersal and allow for a compact Golgi, similar to normal RASSF1A expressing cells. Moreover, we found that loss of RASSF1A correlated with a decrease

in the directional persistence of siRNA treated cells. This reduced directionality was similar to cell migration patterns exhibited by RASSF1A-deficient cancer cells. Interestingly, this loss of directionality also associated with changes in cell polarity. Cells that were either depleted of RASSF1A or were RASSF1A-null exhibited a more rounded, amorphous shape, as compared to control or RASSF1A-transfected cells. Based upon these studies, we draw a model whereby RASSF1A localizes segmentally within the MT network and also at the Golgi. These localizations allow for proper organization of the Golgi and alteration of the MT network that allow for the establishment of a polarized cell, thus, allowing for directional migration. The local bundling and stabilization capacity of RASSF1A also participates in establishing stable tracks upon which directional trafficking can occur.

In Chapter III, I elucidate the exact mechanism of c-Src trafficking in vascular smooth muscle cells. This work stems from an observation that c-Src vesicle movement is not inhibited by depolymerization of MTs, in addition to discrepancies in the literature concerning the true nature of c-Src trafficking. Currently, conflicting work exists that implicates both the MT and actin cytoskeleton in properly trafficking and localizing c-Src Therefore, determining the mechanism of c-Src trafficking is important not only to resolve this discrepancy, but also because it provides the scientific community with druggable targets that can be used to inhibit cancer cell migration and invasion, both of which rely on c-Src. Elevated levels of c-Src expression can mediate the aforementioned processes through phosphorylation of downstream targets that allow for the formation of actin-based degradative structures, podosomes. Due to c-Src being

highly important for phosphorylation of normal and cancer-related targets, we hypothesized that the cell would utilize many mechanism of regulation to correctly localize it within the cell to prevent aberrant signaling, and that this localization would rely on both the MT and actin cytoskeleton. Thus far, we have determined that long-range, bidirectional trafficking of c-Src is mediated by the MT network; however, in response to MT depolymerization, actin-based motility of c-Src vesicles can occur in a faster, but less directional manner. The formation of these actin comet tails at c-Src vesicle membranes seems to be dependent on the MT-regulated GEF, GEF-H1. We see MT depolymerization can double the amount of actin comet tails at vesicle membranes, however, inhibition of GEF-H1 activity significantly reduces this formation to levels even below non-treated controls. However, constitutive activation of GEF-H1 can induce actin comet tail formation even in the presence of MTs, similar to levels seen in nocodazole treated controls. Furthermore, we also see that RhoB, a Rho GTPase implicated in being important for actin-mediated trafficking of c-Src, is also bidirectionally trafficked along MTs. Not surprisingly, we also find that RhoB localizes to c-Src vesicle membranes, potentially to mediate actin comet tail formation. We further confirmed this molecular mechanism by examining the activation status of RhoB in response to MT depolymerization. Our results show that RhoB activation becomes significantly higher upon MT depolymerization as compared to non-treated control. Based upon these results, we propose a model whereby c-Src can be bidirectionally trafficked MTs, but in response to some cellular cue or dynamic instability, GEF-H1 is released from depolymerizing MTs, thus allowing it to interact with and activate RhoB at c-Src vesicle membranes. This activation would provide the necessary force for c-Src

vesicle fusion with the plasma membrane. Studies are ongoing to determine the functional consequence on podosome formation if we modulate or interrupt this molecular pathway.

In sum, these studies provide a detailed analysis on the function of RASSF1A. Functionally, we have determined that RASSF1A is critical for proper Golgi organization and cell polarity, as well as proper MT dynamics. All of these functions contribute to cellular polarization and development of an asymmetric MT array that is required for cell migration. Additionally, we have identified a molecular mechanism for c-Src trafficking that requires the coordinated efforts of both the MT and actin network. This cytoskeletal crosstalk is crucial for prevention of mislocalization of c-Src and irregular signaling by c-Src. Collectively, these two bodies of work present a mechanism whereby modulation of MT dynamics by MAPs, specifically RASSF1A can serve to regulate c-Src trafficking in cells.

Future Directions

Determine the mechanism of RASSF1A localization to MTs

Our data indicates the RASSF1A utilizes a unique localization within the MT network that can regulate MT dynamics and organization (Arnette *et al.*, 2014). The mechanistic details of how RASSF1A incorporates within the MT network are still unclear. Based on our studies, we know that RASSF1A is associated with MTs within the Golgi region, however, whether RASSF1A at the Golgi is capable of providing structural support by incorporating into the nascent protofilaments or forms a collar

around the MT as it polymerizes is an area that requires further examination. To address the association of RASSF1A with MTs, we will utilize live-cell imaging in combination with nocodazole washout experiments to examine MT nucleation at the Golgi. This will allow us to assess whether nascent MTs incorporate RASSF1A as the MT polymerizes. These nocodazole washout experiments can be performed with 2-color live-cell imaging to image MTs and RASSF1A simultaneously. In order to determine if RASSF1A forms a collar around polymerized MTs, conventional electron microscopy and/or cry-em will be used to determine the higher order structure of purified RASSF1A. Additionally, it may be that RASSF1A localization may also be regulated by and/or induce alterations in the structure of protofilaments to increase RASSF1A binding affinity at specific sites. The structure of purified tubulin, repolymerized in the presence or absence of purified RASSF1A protein will be examined by electron microscopy.

Determine RASSF1A domain responsible for MT association and bundling

Revealing the domain responsible for MT association and bundling is critical to understanding how RASSF1A can exert its influence on the MT network. RASSF1A is capable of both homo- and heterotypic interaction, both with itself and other RASSF family members (Ortiz-Vega *et al.*, 2002). We have found that MT association is a key factor in the ability of RASSF1A to exert its function on MT dynamics and that MT bundling and stabilization is crucial for the formation of an organized Golgi structure and for cell polarity (Arnette *et al.*, 2014), therefore, determining the protein-protein interaction domains may provide useful insight into how RASSF1A regulates Golgi

formation and cell polarity. To determine the domain responsible for MT association and bundling, several truncation mutations of wild-type RASSF1A protein will be combined with live-cell imaging techniques, as well as immunohistochemistry. Subsequently, analysis of MT bundling upon expression of various truncation mutations will be used to determine the RASSF1A domain(s) necessary to mediate association and bundling.

Determine if cytoskeletal crosstalk in c-Src trafficking is an independent or combinatorial process

Our data indicate that c-Src vesicular trafficking relies on both the MT and actin network for proper positioning of c-Src. However, it is not clear whether these are two independent mechanisms that have evolutionarily converged to increase the efficiency of c-Src trafficking, or whether these are two redundant processes. Since we see actin polymerization localized to c-Src vesicle membranes in the presence of MTs, we hypothesize that this localization may serve to enhance c-Src vesicular trafficking along MTs, and in the absence of MTs, serves as a mechanism to deliver c-Src vesicles to the plasma membrane. To test if this is a convergent mechanism, triple-color live-cell imaging of cells expressing c-Src, cortactin, and a MT marker, EMTB, will be performed. As non-treated control cells do exhibit some actin polymerization at c-Src vesicle membranes, live-cell imaging of cells expressing the three aforementioned constructs will be used for analysis. Velocity analysis of c-Src vesicles that do exhibit actin polymerization in the presence of MTs will be compared to non-actin-associated vesicles to determine any added effects that this polymerization may have on vesicle delivery. Directionality of these vesicles will also be assessed to determine if they

exhibit increased directional persistence as compared to their non-actin-associated counterparts. Analysis will be performed through manual tracking of c-Src vesicle utilizing ImageJ software to detect vesicle movement throughout the length of the imaging sequence.

Determine the effect of GEF-H1 inhibition on cortactin association and RhoB activation

As we have demonstrated, MT depolymerization can lead to activation of RhoB in cells. Whether or not this activation is dependent upon the Rho GEF, GEF-H1 has yet to be determined. In order to further implicate GEF-H1 in this pathway, expression of various GEF-H1 constructs (GEF-WT, GEF-DN, GEF-CA) will be combined with immunohistochemistry and triple-color live cell imaging. The formation of actin comet tails in immunohistochemistry samples will be scored via similar methods as reported in (Arnette *et al.*, 2014). In order to assess association of cortactin with c-Src vesicles after expression of various GEF-H1 constructs, mcherry-Src will be re-cloned into a Cy2-fluorescent tag, and triple-color imaging will be utilized in control and nocodazole-treatment conditions. The JaCoP plug-in of ImageJ will then be used to calculate cortactin association. Additionally, RhoB activation in cells expressing various GEF-H1 constructs will be assessed via RBD-RhoB pulldown and western blotting both in the presence and absence of MTs.

Determine the functional consequence of inhibition of GEF-H1-mediated cytoskeletal crosstalk

As mentioned earlier, the c-Src serves to regulate several key processes within the cell. One important process that c-Src regulates is the formation of podosomes, actin-based degradative structures found in a variety of cell types (Berdeaux *et al.*, 2004; Gatesman *et al.*, 2004; Tatin *et al.*, 2006). Formation of these structures can have both detrimental and beneficial effects. For example, in osteoclasts, podosomes are necessary for bone resorption and remodeling (Destaing *et al.*, 2008), but podosome formation can also contribute to disease by enhancing tumor cell migration (Yamaguchi *et al.*, 2006) or invasion of VMSCs into atherosclerotic plaques (Mak, 2011). Our data indicates that the proper positioning of c-Src requires both MTs and actin for proper positioning, however, how this relates to c-Src function is yet to be resolved. To address this, we will first test the efficiency of podosome formation in the presence and absence of MTs. To further implicate GEF-H1 as a druggable target that may interfere with podosome formation, we will inhibit GEF-H1 activity through siRNA depletion or expression of a GEF-H1 dominant-negative construct and assess the formation of podosomes within these cells. We will be able to utilize podosome formation as a read-out of whether or not c-Src mislocalization has any affect on subcellular structure formation. Podosome formation will be stimulated through pretreatment of cells with phorbol esters and cells will then be immediately fixed and stained for podosomal proteins, such as cortactin. Analysis of the number of podosomes as well as their location of formation will be determined and assessed visually and with ImageJ software to quantify the percent area occupied by podosomes. Immunofluorescence studies will

also be combined with biochemical assays (western blot) to determine the amount of activated Src under these conditions.

Determine the location of c-Src activation

As mentioned, c-Src is normally found inactive within the perinuclear region (Radziwill *et al.*, 2007; Walker *et al.*, 2007); however, upon stimulation c-Src must be activated to interact with downstream effectors. Currently, the spatiotemporal activation of c-Src is unknown. It is reasonable to think that c-Src activation would occur within the perinuclear region or as c-Src is being trafficked out to the cell periphery; however, we assume that this sort of activation would allow for aberrant signaling as c-Src can then interact with a variety of perinuclear and cytoplasmic effector proteins, thus potentially leading to their activation. Therefore, we hypothesize that c-Src is locally activated at the plasma membrane to regulate c-Src activation of target effectors. In order to determine the precise location of c-Src activation, cells will be microinjected with a fluorescently labeled c-Src-specific biosensor (Gulyani *et al.*, 2011) and imaged by differential interference contrast (DIC). From these live-cell image sequences, ratio images of non-stimulated and phorbol ester treated cells will be created. Ratio images correlated to biosensor activation will be created through automatic line scanning software.

REFERENCES

Alvarez, R.H., Kantarjian, H.M., and Cortes, J.E. (2006). The role of Src in solid and hematologic malignancies: development of new-generation Src inhibitors. Cancer *107*, 1918-1929.

Arnal, I., Karsenti, E., and Hyman, A.A. (2000). Structural transitions at microtubule ends correlate with their dynamic properties in Xenopus egg extracts. The Journal of cell biology *149*, 767-774.

Arnette, C., Efimova, N., Zhu, X., Clark, G.J., and Kaverina, I. (2014). Microtubule segment stabilization by RASSF1A is required for proper microtubule dynamics and Golgi integrity. Molecular biology of the cell.

Baines, A.J., and Bennett, V. (1986). Synapsin I is a microtubule-bundling protein. Nature *319*, 145-147.

Baksh, S., Tommasi, S., Fenton, S., Yu, V.C., Martins, L.M., Pfeifer, G.P., Latif, F., Downward, J., and Neel, B.G. (2005). The tumor suppressor RASSF1A and MAP-1 link death receptor signaling to Bax conformational change and cell death. Mol Cell *18*, 637-650.

Berdeaux, R.L., Diaz, B., Kim, L., and Martin, G.S. (2004). Active Rho is localized to podosomes induced by oncogenic Src and is required for their assembly and function. The Journal of cell biology *166*, 317-323.

Bershadsky, A.D., and Futerman, A.H. (1994). Disruption of the Golgi apparatus by brefeldin A blocks cell polarization and inhibits directed cell migration. Proceedings of the National Academy of Sciences of the United States of America *91*, 5686-5689.

Berta, A.I., Boesze-Battaglia, K., Magyar, A., Szel, A., and Kiss, A.L. (2011). Localization of caveolin-1 and c-src in mature and differentiating photoreceptors: raft proteins co-distribute with rhodopsin during development. Journal of molecular histology *42*, 523-533.

Birkenfeld, J., Nalbant, P., Bohl, B.P., Pertz, O., Hahn, K.M., and Bokoch, G.M. (2007). GEF-H1 modulates localized RhoA activation during cytokinesis under the control of mitotic kinases. Developmental cell *12*, 699-712.

Birkenfeld, J., Nalbant, P., Yoon, S.H., and Bokoch, G.M. (2008). Cellular functions of GEF-H1, a microtubule-regulated Rho-GEF: is altered GEF-H1 activity a crucial determinant of disease pathogenesis? Trends in cell biology *18*, 210-219.

Biscardi, J.S., Tice, D.A., and Parsons, S.J. (1999). c-Src, receptor tyrosine kinases, and human cancer. Advances in cancer research *76*, 61-119.

Bjorge, J.D., Jakymiw, A., and Fujita, D.J. (2000). Selected glimpses into the activation and function of Src kinase. Oncogene *19*, 5620-5635.

Boateng, L.R., Cortesio, C.L., and Huttenlocher, A. (2012). Src-mediated phosphorylation of mammalian Abp1 (DBNL) regulates podosome rosette formation in transformed fibroblasts. Journal of cell science *125*, 1329-1341.

Bretscher, A. (2005). Microtubule tips redirect actin assembly. Developmental cell *8*, 458-459.

Brum Cde, A., Duarte, I.D., Webb, R.C., and Leite, R. (2005). Disruption of microtubular network attenuates histamine-induced dilation in rat mesenteric vessels. American journal of physiology. Cell physiology *288*, C443-449.

Bu, W., Lim, K.B., Yu, Y.H., Chou, A.M., Sudhaharan, T., and Ahmed, S. (2010). Cdc42 interaction with N-WASP and Toca-1 regulates membrane tubulation, vesicle formation and vesicle motility: implications for endocytosis. PloS one *5*, e12153.

Burbee, D.G., Forgacs, E., Zochbauer-Muller, S., Shivakumar, L., Fong, K., Gao, B., Randle, D., Kondo, M., Virmani, A., Bader, S., Sekido, Y., Latif, F., Milchgrub, S., Toyooka, S., Gazdar, A.F., Lerman, M.I., Zabarovsky, E., White, M., and Minna, J.D. (2001). Epigenetic inactivation of RASSF1A in lung and breast cancers and malignant phenotype suppression. Journal of the National Cancer Institute *93*, 691-699.

Burkhardt, J.K., Echeverri, C.J., Nilsson, T., and Vallee, R.B. (1997). Overexpression of the dynamitin (p50) subunit of the dynactin complex disrupts dynein-dependent maintenance of membrane organelle distribution. The Journal of cell biology *139*, 469-484.

Cai, D., McEwen, D.P., Martens, J.R., Meyhofer, E., and Verhey, K.J. (2009). Single molecule imaging reveals differences in microtubule track selection between Kinesin motors. PLoS Biol *7*, e1000216.

Cameron, L.A., Footer, M.J., van Oudenaarden, A., and Theriot, J.A. (1999). Motility of ActA protein-coated microspheres driven by actin polymerization. Proceedings of the National Academy of Sciences of the United States of America *96*, 4908-4913.

Cao, H., Chen, J., Krueger, E.W., and McNiven, M.A. (2010). SRC-mediated phosphorylation of dynamin and cortactin regulates the "constitutive" endocytosis of transferrin. Molecular and cellular biology *30*, 781-792.

Carlier, M.F., Didry, D., and Pantaloni, D. (1997). Hydrolysis of GTP associated with the formation of tubulin oligomers is involved in microtubule nucleation. Biophysical journal *73*, 418-427.

Cassimeris, L., and Spittle, C. (2001). Regulation of microtubule-associated proteins. International review of cytology *210*, 163-226.

Cerione, R.A., and Zheng, Y. (1996). The Dbl family of oncogenes. Current opinion in cell biology *8*, 216-222.

Chabin-Brion, K., Marceiller, J., Perez, F., Settegrana, C., Drechou, A., Durand, G., and Pous, C. (2001). The Golgi complex is a microtubule-organizing organelle. Molecular biology of the cell *12*, 2047-2060.

Chang, Y.C., Nalbant, P., Birkenfeld, J., Chang, Z.F., and Bokoch, G.M. (2008). GEF-H1 couples nocodazole-induced microtubule disassembly to cell contractility via RhoA. Molecular biology of the cell *19*, 2147-2153.

Chen, J., Kanai, Y., Cowan, N.J., and Hirokawa, N. (1992). Projection domains of MAP2 and tau determine spacings between microtubules in dendrites and axons. Nature *360*, 674-677.

Chen, S., Chen, J., Shi, H., Wei, M., Castaneda-Castellanos, D.R., Bultje, R.S., Pei, X., Kriegstein, A.R., Zhang, M., and Shi, S.H. (2013). Regulation of microtubule stability and organization by mammalian Par3 in specifying neuronal polarity. Developmental cell *24*, 26-40.

Chow, L.S., Lo, K.W., Kwong, J., To, K.F., Tsang, K.S., Lam, C.W., Dammann, R., and Huang, D.P. (2004). RASSF1A is a target tumor suppressor from 3p21.3 in nasopharyngeal carcinoma. International journal of cancer. Journal international du cancer *109*, 839-847.

Cole, D.G., Chinn, S.W., Wedaman, K.P., Hall, K., Vuong, T., and Scholey, J.M. (1993). Novel heterotrimeric kinesin-related protein purified from sea urchin eggs. Nature *366*, 268-270.

Cole, N.B., Sciaky, N., Marotta, A., Song, J., and Lippincott-Schwartz, J. (1996). Golgi dispersal during microtubule disruption: regeneration of Golgi stacks at peripheral endoplasmic reticulum exit sites. Molecular biology of the cell *7*, 631-650.

Dallol, A., Agathanggelou, A., Fenton, S.L., Ahmed-Choudhury, J., Hesson, L., Vos, M.D., Clark, G.J., Downward, J., Maher, E.R., and Latif, F. (2004). RASSF1A interacts with microtubule-associated proteins and modulates microtubule dynamics. Cancer research *64*, 4112-4116.

Dallol, A., Agathanggelou, A., Tommasi, S., Pfeifer, G.P., Maher, E.R., and Latif, F. (2005). Involvement of the RASSF1A tumor suppressor gene in controlling cell migration. Cancer research *65*, 7653-7659.

Dallol, A., Hesson, L.B., Matallanas, D., Cooper, W.N., O'Neill, E., Maher, E.R., Kolch, W., and Latif, F. (2009). RAN GTPase is a RASSF1A effector involved in controlling microtubule organization. Curr Biol *19*, 1227-1232.

Dammann, R., Li, C., Yoon, J.H., Chin, P.L., Bates, S., and Pfeifer, G.P. (2000). Epigenetic inactivation of a RAS association domain family protein from the lung tumour suppressor locus 3p21.3. Nature genetics *25*, 315-319.

Daub, H., Gevaert, K., Vandekerckhove, J., Sobel, A., and Hall, A. (2001). Rac/Cdc42 and p65PAK regulate the microtubule-destabilizing protein stathmin through phosphorylation at serine 16. The Journal of biological chemistry *276*, 1677-1680.

De Luca, A., D'Alessio, A., Gallo, M., Maiello, M.R., Bode, A.M., and Normanno, N. (2014). Src and CXCR4 are involved in the invasiveness of breast cancer cells with acquired resistance to lapatinib. Cell cycle *13*, 148-156.

Destaing, O., Sanjay, A., Itzstein, C., Horne, W.C., Toomre, D., De Camilli, P., and Baron, R. (2008). The tyrosine kinase activity of c-Src regulates actin dynamics and organization of podosomes in osteoclasts. Molecular biology of the cell *19*, 394-404.

Donepudi, M., and Resh, M.D. (2008). c-Src trafficking and co-localization with the EGF receptor promotes EGF ligand-independent EGF receptor activation and signaling. Cellular signalling *20*, 1359-1367.

Donninger, H., Vos, M.D., and Clark, G.J. (2007). The RASSF1A tumor suppressor. J Cell Sci *120*, 3163-3172.

Drabek, K., van Ham, M., Stepanova, T., Draegestein, K., van Horssen, R., Sayas, C.L., Akhmanova, A., Ten Hagen, T., Smits, R., Fodde, R., Grosveld, F., and Galjart, N. (2006). Role of CLASP2 in microtubule stabilization and the regulation of persistent motility. Curr Biol *16*, 2259-2264.

Dreijerink, K., Braga, E., Kuzmin, I., Geil, L., Duh, F.M., Angeloni, D., Zbar, B., Lerman, M.I., Stanbridge, E.J., Minna, J.D., Protopopov, A., Li, J., Kashuba, V., Klein, G., and Zabarovsky, E.R. (2001). The candidate tumor suppressor gene, RASSF1A, from human chromosome 3p21.3 is involved in kidney tumorigenesis. Proceedings of the National Academy of Sciences of the United States of America *98*, 7504-7509.

El-Kalla, M., Onyskiw, C., and Baksh, S. (2010). Functional importance of RASSF1A microtubule localization and polymorphisms. Oncogene *29*, 5729-5740.

Ezratty, E.J., Partridge, M.A., and Gundersen, G.G. (2005). Microtubule-induced focal adhesion disassembly is mediated by dynamin and focal adhesion kinase. Nature cell biology *7*, 581-590.

Faire, K., Waterman-Storer, C.M., Gruber, D., Masson, D., Salmon, E.D., and Bulinski, J.C. (1999). E-MAP-115 (ensconsin) associates dynamically with microtubules in vivo and is not a physiological modulator of microtubule dynamics. Journal of cell science *112 (Pt 23)*, 4243-4255.

Fukata, Y., Amano, M., and Kaibuchi, K. (2001). Rho-Rho-kinase pathway in smooth muscle contraction and cytoskeletal reorganization of non-muscle cells. Trends in pharmacological sciences *22*, 32-39.

Gatesman, A., Walker, V.G., Baisden, J.M., Weed, S.A., and Flynn, D.C. (2004). Protein kinase Calpha activates c-Src and induces podosome formation via AFAP-110. Molecular and cellular biology *24*, 7578-7597.

Gulyani, A., Vitriol, E., Allen, R., Wu, J., Gremyachinskiy, D., Lewis, S., Dewar, B., Graves, L.M., Kay, B.K., Kuhlman, B., Elston, T., and Hahn, K.M. (2011). A biosensor generated via high-throughput screening quantifies cell edge Src dynamics. Nature chemical biology *7*, 437-444.

Gundersen, G.G., Gomes, E.R., and Wen, Y. (2004). Cortical control of microtubule stability and polarization. Current opinion in cell biology *16*, 106-112.

Guo, C., Tommasi, S., Liu, L., Yee, J.K., Dammann, R., and Pfeifer, G.P. (2007). RASSF1A is part of a complex similar to the Drosophila Hippo/Salvador/Lats tumor-suppressor network. Curr Biol *17*, 700-705.

Guo, F., Debidda, M., Yang, L., Williams, D.A., and Zheng, Y. (2006). Genetic deletion of Rac1 GTPase reveals its critical role in actin stress fiber formation and focal adhesion complex assembly. The Journal of biological chemistry *281*, 18652-18659.

Hall, D.H., and Hedgecock, E.M. (1991). Kinesin-related gene unc-104 is required for axonal transport of synaptic vesicles in C. elegans. Cell *65*, 837-847.

Hall, K., Cole, D.G., Yeh, Y., Scholey, J.M., and Baskin, R.J. (1993). Force-velocity relationships in kinesin-driven motility. Nature *364*, 457-459.

Hanahan, D., and Weinberg, R.A. (2000). The hallmarks of cancer. Cell *100*, 57-70.

Harris, T.J., and Peifer, M. (2007). aPKC controls microtubule organization to balance adherens junction symmetry and planar polarity during development. Developmental cell *12*, 727-738.

Heck, J.N., Ponik, S.M., Garcia-Mendoza, M.G., Pehlke, C.A., Inman, D.R., Eliceiri, K.W., and Keely, P.J. (2012). Microtubules regulate GEF-H1 in response to extracellular matrix stiffness. Molecular biology of the cell *23*, 2583-2592.

Herman, J.G., and Baylin, S.B. (2003). Gene silencing in cancer in association with promoter hypermethylation. The New England journal of medicine *349*, 2042-2054.

Hesson, L., Bieche, I., Krex, D., Criniere, E., Hoang-Xuan, K., Maher, E.R., and Latif, F. (2004). Frequent epigenetic inactivation of RASSF1A and BLU genes located within the critical 3p21.3 region in gliomas. Oncogene *23*, 2408-2419.

Hirokawa, N. (1998). Kinesin and dynein superfamily proteins and the mechanism of organelle transport. Science *279*, 519-526.

Hirschberg, K., Miller, C.M., Ellenberg, J., Presley, J.F., Siggia, E.D., Phair, R.D., and Lippincott-Schwartz, J. (1998). Kinetic analysis of secretory protein traffic and characterization of golgi to plasma membrane transport intermediates in living cells. The Journal of cell biology *143*, 1485-1503.

Hori, Y., Kikuchi, A., Isomura, M., Katayama, M., Miura, Y., Fujioka, H., Kaibuchi, K., and Takai, Y. (1991). Post-translational modifications of the C-terminal region of the rho protein are important for its interaction with membranes and the stimulatory and inhibitory GDP/GTP exchange proteins. Oncogene *6*, 515-522.

Horne, W.C., Neff, L., Chatterjee, D., Lomri, A., Levy, J.B., and Baron, R. (1992). Osteoclasts express high levels of pp60c-src in association with intracellular membranes. The Journal of cell biology *119*, 1003-1013.

Imamura, H., Takaishi, K., Nakano, K., Kodama, A., Oishi, H., Shiozaki, H., Monden, M., Sasaki, T., and Takai, Y. (1998). Rho and Rab small G proteins coordinately reorganize stress fibers and focal adhesions in MDCK cells. Molecular biology of the cell *9*, 2561-2575.

Irby, R.B., Mao, W., Coppola, D., Kang, J., Loubeau, J.M., Trudeau, W., Karl, R., Fujita, D.J., Jove, R., and Yeatman, T.J. (1999). Activating SRC mutation in a subset of advanced human colon cancers. Nature genetics *21*, 187-190.

Irby, R.B., and Yeatman, T.J. (2000). Role of Src expression and activation in human cancer. Oncogene *19*, 5636-5642.

Jesuthasan, S., and Stahle, U. (1997). Dynamic microtubules and specification of the zebrafish embryonic axis. Current biology : CB *7*, 31-42.

Jo, H., Kim, J.W., Kang, G.H., Park, N.H., Song, Y.S., Kang, S.B., and Lee, H.P. (2006). Association of promoter hypermethylation of the RASSF1A gene with prognostic parameters in endometrial cancer. Oncol Res *16*, 205-209.

Jones, P.A., and Baylin, S.B. (2002). The fundamental role of epigenetic events in cancer. Nature reviews. Genetics *3*, 415-428.

Jung, H.Y., Jung, J.S., Whang, Y.M., and Kim, Y.H. (2013). RASSF1A Suppresses Cell Migration through Inactivation of HDAC6 and Increase of Acetylated alpha-Tubulin. Cancer research and treatment : official journal of Korean Cancer Association *45*, 134-144.

Kadir, S., Astin, J.W., Tahtamouni, L., Martin, P., and Nobes, C.D. (2011). Microtubule remodelling is required for the front-rear polarity switch during contact inhibition of locomotion. J Cell Sci *124*, 2642-2653.

Kamon, H., Kawabe, T., Kitamura, H., Lee, J., Kamimura, D., Kaisho, T., Akira, S., Iwamatsu, A., Koga, H., Murakami, M., and Hirano, T. (2006). TRIF-GEFH1-RhoB pathway is involved in MHCII expression on dendritic cells that is critical for CD4 T-cell activation. The EMBO journal *25*, 4108-4119.

Kang, G.H., Lee, S., Lee, H.J., and Hwang, K.S. (2004). Aberrant CpG island hypermethylation of multiple genes in prostate cancer and prostatic intraepithelial neoplasia. J Pathol *202*, 233-240.

Kaplan, K.B., Swedlow, J.R., Varmus, H.E., and Morgan, D.O. (1992). Association of p60c-src with endosomal membranes in mammalian fibroblasts. The Journal of cell biology *118*, 321-333.

Katoh, K., Kano, Y., and Noda, Y. (2011). Rho-associated kinase-dependent contraction of stress fibres and the organization of focal adhesions. Journal of the Royal Society, Interface / the Royal Society *8*, 305-311.

Kaverina, I., Krylyshkina, O., and Small, J.V. (1999). Microtubule targeting of substrate contacts promotes their relaxation and dissociation. J Cell Biol *146*, 1033-1044.

Kawano, Y., Yoshimura, T., and Kaibuchi, K. (2002). Smooth muscle contraction by small GTPase Rho. Nagoya journal of medical science *65*, 1-8.

Kellokumpu, S., Sormunen, R., and Kellokumpu, I. (2002). Abnormal glycosylation and altered Golgi structure in colorectal cancer: dependence on intra-Golgi pH. FEBS Lett *516*, 217-224.

Kim, M.S., Kim, G.M., Choi, Y.J., Kim, H.J., Kim, Y.J., and Jin, W. (2013). c-Src activation through a TrkA and c-Src interaction is essential for cell proliferation and hematological malignancies. Biochemical and biophysical research communications *441*, 431-437.

Kim, S.T., Lim, D.S., Canman, C.E., and Kastan, M.B. (1999). Substrate specificities and identification of putative substrates of ATM kinase family members. The Journal of biological chemistry *274*, 37538-37543.

Kirschner, M.W., and Mitchison, T. (1986). Microtubule dynamics. Nature *324*, 621.

Krendel, M., Zenke, F.T., and Bokoch, G.M. (2002). Nucleotide exchange factor GEF-H1 mediates cross-talk between microtubules and the actin cytoskeleton. Nature cell biology *4*, 294-301.

Kupfer, A., Dennert, G., and Singer, S.J. (1983). Polarization of the Golgi apparatus and the microtubule-organizing center within cloned natural killer cells bound to their targets. Proc Natl Acad Sci U S A *80*, 7224-7228.

Kuzmin, I., Gillespie, J.W., Protopopov, A., Geil, L., Dreijerink, K., Yang, Y., Vocke, C.D., Duh, F.M., Zabarovsky, E., Minna, J.D., Rhim, J.S., Emmert-Buck, M.R., Linehan, W.M., and Lerman, M.I. (2002). The RASSF1A tumor suppressor gene is inactivated in prostate tumors and suppresses growth of prostate carcinoma cells. Cancer research *62*, 3498-3502.

Lee, M.G., Kim, H.Y., Byun, D.S., Lee, S.J., Lee, C.H., Kim, J.I., Chang, S.G., and Chi, S.G. (2001). Frequent epigenetic inactivation of RASSF1A in human bladder carcinoma. Cancer Res *61*, 6688-6692.

Lee, S., Han, J.W., Leeper, L., Gruver, J.S., and Chung, C.Y. (2009). Regulation of the formation and trafficking of vesicles from Golgi by PCH family proteins during chemotaxis. Biochim Biophys Acta *1793*, 1199-1209.

Leite, R., and Webb, R.C. (1998). Microtubule disruption potentiates phenylephrine-induced vasoconstriction in rat mesenteric arterial bed. European journal of pharmacology *351*, R1-3.

Lerman, M.I., and Minna, J.D. (2000). The 630-kb lung cancer homozygous deletion region on human chromosome 3p21.3: identification and evaluation of the resident candidate tumor suppressor genes. The International Lung Cancer Chromosome 3p21.3 Tumor Suppressor Gene Consortium. Cancer research *60*, 6116-6133.

Liu, B.P., Chrzanowska-Wodnicka, M., and Burridge, K. (1998). Microtubule depolymerization induces stress fibers, focal adhesions, and DNA synthesis via the GTP-binding protein Rho. Cell adhesion and communication *5*, 249-255.

Liu, L., Amy, V., Liu, G. and McKeehan, W. L. (2002). Specificity of the methylation suppressed A isoform of candidate tumor suppressor RASSF1 for microtubule hyperstabilization is determined by cell death inducer C19ORF5. Cancer research *65*, 1830-1838.

Liu, L., Broaddus, R.R., Yao, J.C., Xie, S., White, J.A., Wu, T.T., Hamilton, S.R., and Rashid, A. (2005). Epigenetic alterations in neuroendocrine tumors: methylation of RAS-association domain family 1, isoform A and p16 genes are associated with metastasis. Mod Pathol *18*, 1632-1640.

Liu, L., Tommasi, S., Lee, D.H., Dammann, R., and Pfeifer, G.P. (2003). Control of microtubule stability by the RASSF1A tumor suppressor. Oncogene *22*, 8125-8136.

Magdalena, J., Millard, T.H., and Machesky, L.M. (2003). Microtubule involvement in NIH 3T3 Golgi and MTOC polarity establishment. Journal of cell science *116*, 743-756.

Mak, A.S. (2011). p53 regulation of podosome formation and cellular invasion in vascular smooth muscle cells. Cell adhesion & migration *5*, 144-149.

Mandelkow, E., and Mandelkow, E.M. (1995). Microtubules and microtubule-associated proteins. Current opinion in cell biology *7*, 72-81.

Manneville, J.B., Jehanno, M., and Etienne-Manneville, S. (2010). Dlg1 binds GKAP to control dynein association with microtubules, centrosome positioning, and cell polarity. The Journal of cell biology *191*, 585-598.

Margolis, R.L. (1981). Role of GTP hydrolysis in microtubule treadmilling and assembly. Proceedings of the National Academy of Sciences of the United States of America *78*, 1586-1590.

Marx, A., Muller, J., and Mandelkow, E. (2005). The structure of microtubule motor proteins. Advances in protein chemistry *71*, 299-344.

Mattie, F.J., Stackpole, M.M., Stone, M.C., Clippard, J.R., Rudnick, D.A., Qiu, Y., Tao, J., Allender, D.L., Parmar, M., and Rolls, M.M. (2010). Directed microtubule growth, +TIPs, and kinesin-2 are required for uniform microtubule polarity in dendrites. Current biology : CB *20*, 2169-2177.

Michaelson, D., Silletti, J., Murphy, G., D'Eustachio, P., Rush, M., and Philips, M.R. (2001). Differential localization of Rho GTPases in live cells: regulation by hypervariable regions and RhoGDI binding. The Journal of cell biology *152*, 111-126.

Miller, P.M., Folkmann, A.W., Maia, A.R., Efimova, N., Efimov, A., and Kaverina, I. (2009). Golgi-derived CLASP-dependent microtubules control Golgi organization and polarized trafficking in motile cells. Nature cell biology *11*, 1069-1080.

Mimori-Kiyosue, Y., Grigoriev, I., Lansbergen, G., Sasaki, H., Matsui, C., Severin, F., Galjart, N., Grosveld, F., Vorobjev, I., Tsukita, S., and Akhmanova, A. (2005). CLASP1 and CLASP2 bind to EB1 and regulate microtubule plus-end dynamics at the cell cortex. J Cell Biol *168*, 141-153.

Mitchison, T., and Kirschner, M. (1984). Dynamic instability of microtubule growth. Nature *312*, 237-242.

Miyazaki, T., Sanjay, A., Neff, L., Tanaka, S., Horne, W.C., and Baron, R. (2004). Src kinase activity is essential for osteoclast function. The Journal of biological chemistry *279*, 17660-17666.

Mollinari, C., Kleman, J.P., Jiang, W., Schoehn, G., Hunter, T., and Margolis, R.L. (2002). PRC1 is a microtubule binding and bundling protein essential to maintain the mitotic spindle midzone. J Cell Biol *157*, 1175-1186.

Muller, H.M., Widschwendter, A., Fiegl, H., Ivarsson, L., Goebel, G., Perkmann, E., Marth, C., and Widschwendter, M. (2003). DNA methylation in serum of breast cancer patients: an independent prognostic marker. Cancer Res *63*, 7641-7645.

Musch, A. (2004). Microtubule organization and function in epithelial cells. Traffic *5*, 1-9.

Newton, A.C. (1995). Protein kinase C: structure, function, and regulation. The Journal of biological chemistry *270*, 28495-28498.

Nguyen, H.L., Chari, S., Gruber, D., Lue, C.M., Chapin, S.J., and Bulinski, J.C. (1997). Overexpression of full- or partial-length MAP4 stabilizes microtubules and alters cell growth. J Cell Sci *110 (Pt 2)*, 281-294.

Noritake, J., Watanabe, T., Sato, K., Wang, S., and Kaibuchi, K. (2005). IQGAP1: a key regulator of adhesion and migration. Journal of cell science *118*, 2085-2092.

Ortiz-Vega, S., Khokhlatchev, A., Nedwidek, M., Zhang, X.F., Dammann, R., Pfeifer, G.P., and Avruch, J. (2002). The putative tumor suppressor RASSF1A homodimerizes and heterodimerizes with the Ras-GTP binding protein Nore1. Oncogene *21*, 1381-1390.

Pfeifer, G.P., and Dammann, R. (2005). Methylation of the tumor suppressor gene RASSF1A in human tumors. Biochemistry. Biokhimiia *70*, 576-583.

Piperno, G., LeDizet, M., and Chang, X.J. (1987). Microtubules containing acetylated alpha-tubulin in mammalian cells in culture. J Cell Biol *104*, 289-302.

Ponting, C.P., and Benjamin, D.R. (1996). A novel family of Ras-binding domains. Trends in biochemical sciences *21*, 422-425.

Prager-Khoutorsky, M., Goncharov, I., Rabinkov, A., Mirelman, D., Geiger, B., and Bershadsky, A.D. (2007). Allicin inhibits cell polarization, migration and division via its direct effect on microtubules. Cell motility and the cytoskeleton *64*, 321-337.

Praskova, M., Khoklatchev, A., Ortiz-Vega, S., and Avruch, J. (2004). Regulation of the MST1 kinase by autophosphorylation, by the growth inhibitory proteins, RASSF1 and NORE1, and by Ras. Biochem J *381*, 453-462.

Radziwill, G., Weiss, A., Heinrich, J., Baumgartner, M., Boisguerin, P., Owada, K., and Moelling, K. (2007). Regulation of c-Src by binding to the PDZ domain of AF-6. The EMBO journal *26*, 2633-2644.

Rahkila, P., Vaananen, K., Saraste, J., and Metsikko, K. (1997). Endoplasmic reticulum to Golgi trafficking in multinucleated skeletal muscle fibers. Exp Cell Res *234*, 452-464.

Reinecke, J.B., Katafiasz, D., Naslavsky, N., and Caplan, S. (2014). Regulation of Src trafficking and activation by the endocytic regulatory proteins MICAL-L1 and EHD1. Journal of cell science.

Ridley, A.J. (2006). Rho GTPases and actin dynamics in membrane protrusions and vesicle trafficking. Trends in cell biology *16*, 522-529.

Ridley, A.J., Schwartz, M.A., Burridge, K., Firtel, R.A., Ginsberg, M.H., Borisy, G., Parsons, J.T., and Horwitz, A.R. (2003). Cell migration: integrating signals from front to back. Science *302*, 1704-1709.

Roby, K.F., Son, D.S., Taylor, C.C., Montgomery-Rice, V., Kirchoff, J., Tang, S., and Terranova, P.F. (2005). Alterations in reproductive function in SRC tyrosine kinase knockout mice. Endocrine *26*, 169-176.

Rodriguez, O.C., Schaefer, A.W., Mandato, C.A., Forscher, P., Bement, W.M., and Waterman-Storer, C.M. (2003). Conserved microtubule-actin interactions in cell movement and morphogenesis. Nature cell biology *5*, 599-609.

Roghi, C., and Allan, V.J. (1999). Dynamic association of cytoplasmic dynein heavy chain 1a with the Golgi apparatus and intermediate compartment. Journal of cell science *112 (Pt 24)*, 4673-4685.

Rong, R., Jiang, L.Y., Sheikh, M.S., and Huang, Y. (2007). Mitotic kinase Aurora-A phosphorylates RASSF1A and modulates RASSF1A-mediated microtubule interaction and M-phase cell cycle regulation. Oncogene *26*, 7700-7708.

Rong, R., Jin, W., Zhang, J., Sheikh, M.S., and Huang, Y. (2004). Tumor suppressor RASSF1A is a microtubule-binding protein that stabilizes microtubules and induces G2/M arrest. Oncogene *23*, 8216-8230.

Rowning, B.A., Wells, J., Wu, M., Gerhart, J.C., Moon, R.T., and Larabell, C.A. (1997). Microtubule-mediated transport of organelles and localization of beta-catenin to the future dorsal side of Xenopus eggs. Proceedings of the National Academy of Sciences of the United States of America *94*, 1224-1229.

Ryan, S.D., Bhanot, K., Ferrier, A., De Repentigny, Y., Chu, A., Blais, A., and Kothary, R. (2012). Microtubule stability, Golgi organization, and transport flux require dystonin-a2-MAP1B interaction. J Cell Biol *196*, 727-742.

Sahai, E., and Marshall, C.J. (2002). RHO-GTPases and cancer. Nature reviews. Cancer *2*, 133-142.

Sandilands, E., Cans, C., Fincham, V.J., Brunton, V.G., Mellor, H., Prendergast, G.C., Norman, J.C., Superti-Furga, G., and Frame, M.C. (2004). RhoB and actin polymerization coordinate Src activation with endosome-mediated delivery to the membrane. Developmental cell *7*, 855-869.

Sanjay, A., Houghton, A., Neff, L., DiDomenico, E., Bardelay, C., Antoine, E., Levy, J., Gailit, J., Bowtell, D., Horne, W.C., and Baron, R. (2001). Cbl associates with Pyk2 and Src to regulate Src kinase activity, alpha(v)beta(3) integrin-mediated signaling, cell adhesion, and osteoclast motility. The Journal of cell biology *152*, 181-195.

Scheel, H., and Hofmann, K. (2003). A novel interaction motif, SARAH, connects three classes of tumor suppressor. Current biology : CB *13*, R899-900.

Schmoranzer, J., and Simon, S.M. (2003). Role of microtubules in fusion of post-Golgi vesicles to the plasma membrane. Mol Biol Cell *14*, 1558-1569.

Schnapp, B.J. (2003). Trafficking of signaling modules by kinesin motors. Journal of cell science *116*, 2125-2135.

Schnapp, B.J., and Reese, T.S. (1989). Dynein is the motor for retrograde axonal transport of organelles. Proceedings of the National Academy of Sciences of the United States of America *86*, 1548-1552.

Schroer, T.A., Steuer, E.R., and Sheetz, M.P. (1989). Cytoplasmic dynein is a minus end-directed motor for membranous organelles. Cell *56*, 937-946.

Shalloway, D., Coussens, P.M., and Yaciuk, P. (1984). Overexpression of the c-src protein does not induce transformation of NIH 3T3 cells. Proceedings of the National Academy of Sciences of the United States of America *81*, 7071-7075.

Sheetz, M.P. (1996). Microtubule motor complexes moving membranous organelles. Cell structure and function *21*, 369-373.

Shivakumar, L., Minna, J., Sakamaki, T., Pestell, R., and White, M.A. (2002). The RASSF1A tumor suppressor blocks cell cycle progression and inhibits cyclin D1 accumulation. Mol Cell Biol *22*, 4309-4318.

Siegrist, S.E., and Doe, C.Q. (2007). Microtubule-induced cortical cell polarity. Genes & development *21*, 483-496.

Small, J.V., and Kaverina, I. (2003). Microtubules meet substrate adhesions to arrange cell polarity. Current opinion in cell biology *15*, 40-47.

Song, M.S., Chang, J.S., Song, S.J., Yang, T.H., Lee, H., and Lim, D.S. (2005). The centrosomal protein RAS association domain family protein 1A (RASSF1A)-binding protein 1 regulates mitotic progression by recruiting RASSF1A to spindle poles. The Journal of biological chemistry *280*, 3920-3927.

Song, M.S., Song, S.J., Ayad, N.G., Chang, J.S., Lee, J.H., Hong, H.K., Lee, H., Choi, N., Kim, J., Kim, H., Kim, J.W., Choi, E.J., Kirschner, M.W., and Lim, D.S. (2004). The tumour

suppressor RASSF1A regulates mitosis by inhibiting the APC-Cdc20 complex. Nature cell biology *6*, 129-137.

Stewart, R.J., Pesavento, P.A., Woerpel, D.N., and Goldstein, L.S. (1991). Identification and partial characterization of six members of the kinesin superfamily in Drosophila. Proceedings of the National Academy of Sciences of the United States of America *88*, 8470-8474.

Takemura, R., Okabe, S., Umeyama, T., Kanai, Y., Cowan, N.J., and Hirokawa, N. (1992). Increased microtubule stability and alpha tubulin acetylation in cells transfected with microtubule-associated proteins MAP1B, MAP2 or tau. J Cell Sci *103 (Pt 4)*, 953-964.

Takesono, A., Heasman, S.J., Wojciak-Stothard, B., Garg, R., and Ridley, A.J. (2010). Microtubules regulate migratory polarity through Rho/ROCK signaling in T cells. PloS one *5*, e8774.

Tanaka, S., Nohara, T., Iwamoto, M., Sumiyoshi, K., Kimura, K., Takahashi, Y., and Tanigawa, N. (2009). Tau expression and efficacy of paclitaxel treatment in metastatic breast cancer. Cancer Chemother Pharmacol *64*, 341-346.

Tatin, F., Varon, C., Genot, E., and Moreau, V. (2006). A signalling cascade involving PKC, Src and Cdc42 regulates podosome assembly in cultured endothelial cells in response to phorbol ester. Journal of cell science *119*, 769-781.

Thyberg, J., and Moskalewski, S. (1993). Relationship between the Golgi complex and microtubules enriched in detyrosinated or acetylated alpha-tubulin: studies on cells recovering from nocodazole and cells in the terminal phase of cytokinesis. Cell Tissue Res *273*, 457-466.

Timpson, P., Jones, G.E., Frame, M.C., and Brunton, V.G. (2001). Coordination of cell polarization and migration by the Rho family GTPases requires Src tyrosine kinase activity. Current biology : CB *11*, 1836-1846.

Tirnauer, J.S., O'Toole, E., Berrueta, L., Bierer, B.E., and Pellman, D. (1999). Yeast Bim1p promotes the G1-specific dynamics of microtubules. The Journal of cell biology *145*, 993-1007.

Tommasi, S., Dammann, R., Zhang, Z., Wang, Y., Liu, L., Tsark, W.M., Wilczynski, S.P., Li, J., You, M., and Pfeifer, G.P. (2005). Tumor susceptibility of Rassf1a knockout mice. Cancer research *65*, 92-98.

Vale, R.D., Reese, T.S., and Sheetz, M.P. (1985). Identification of a novel force-generating protein, kinesin, involved in microtubule-based motility. Cell *42*, 39-50.

van der Weyden, L., and Adams, D.J. (2007). The Ras-association domain family (RASSF) members and their role in human tumourigenesis. Biochim Biophys Acta *1776*, 58-85.

van der Weyden, L., Tachibana, K.K., Gonzalez, M.A., Adams, D.J., Ng, B.L., Petty, R., Venkitaraman, A.R., Arends, M.J., and Bradley, A. (2005). The RASSF1A isoform of RASSF1 promotes microtubule stability and suppresses tumorigenesis. Molecular and cellular biology *25*, 8356-8367.

van Horck, F.P., Ahmadian, M.R., Haeusler, L.C., Moolenaar, W.H., and Kranenburg, O. (2001). Characterization of p190RhoGEF, a RhoA-specific guanine nucleotide exchange factor that interacts with microtubules. The Journal of biological chemistry *276*, 4948-4956.

Vega, F.M., Colomba, A., Reymond, N., Thomas, M., and Ridley, A.J. (2012). RhoB regulates cell migration through altered focal adhesion dynamics. Open biology *2*, 120076.

Vos, M.D., Dallol, A., Eckfeld, K., Allen, N.P., Donninger, H., Hesson, L.B., Calvisi, D., Latif, F., and Clark, G.J. (2006). The RASSF1A tumor suppressor activates Bax via MOAP-1. The Journal of biological chemistry *281*, 4557-4563.

Vos, M.D., Ellis, C.A., Bell, A., Birrer, M.J., and Clark, G.J. (2000). Ras uses the novel tumor suppressor RASSF1 as an effector to mediate apoptosis. J Biol Chem *275*, 35669-35672.

Vos, M.D., Martinez, A., Elam, C., Dallol, A., Taylor, B.J., Latif, F., and Clark, G.J. (2004). A role for the RASSF1A tumor suppressor in the regulation of tubulin polymerization and genomic stability. Cancer research *64*, 4244-4250.

Walker, V.G., Ammer, A., Cao, Z., Clump, A.C., Jiang, B.H., Kelley, L.C., Weed, S.A., Zot, H., and Flynn, D.C. (2007). PI3K activation is required for PMA-directed activation of cSrc by AFAP-110. American journal of physiology. Cell physiology *293*, C119-132.

Watanabe, T., Noritake, J., and Kaibuchi, K. (2005). Roles of IQGAP1 in cell polarization and migration. Novartis Foundation symposium *269*, 92-101; discussion 101-105, 223-130.

Waterman-Storer, C.M., Worthylake, R.A., Liu, B.P., Burridge, K., and Salmon, E.D. (1999). Microtubule growth activates Rac1 to promote lamellipodial protrusion in fibroblasts. Nature cell biology *1*, 45-50.

Weisenberg, R.C., Deery, W.J., and Dickinson, P.J. (1976). Tubulin-nucleotide interactions during the polymerization and depolymerization of microtubules. Biochemistry *15*, 4248-4254.

Westermann, S., and Weber, K. (2003). Post-translational modifications regulate microtubule function. Nat Rev Mol Cell Biol *4*, 938-947.

Williamson, T., Gordon-Weeks, P.R., Schachner, M., and Taylor, J. (1996). Microtubule reorganization is obligatory for growth cone turning. Proceedings of the National Academy of Sciences of the United States of America *93*, 15221-15226.

Wittmann, T., Bokoch, G.M., and Waterman-Storer, C.M. (2003). Regulation of leading edge microtubule and actin dynamics downstream of Rac1. The Journal of cell biology *161*, 845-851.

Wu, B., Decourt, B., Zabidi, M.A., Wuethrich, L.T., Kim, W.H., Zhou, Z., MacIsaac, K., and Suter, D.M. (2008). Microtubule-mediated Src tyrosine kinase trafficking in neuronal growth cones. Molecular biology of the cell *19*, 4611-4627.

Yadav, S., Puri, S., and Linstedt, A.D. (2009). A primary role for Golgi positioning in directed secretion, cell polarity, and wound healing. Molecular biology of the cell *20*, 1728-1736.

Yamaguchi, H., Pixley, F., and Condeelis, J. (2006). Invadopodia and podosomes in tumor invasion. European journal of cell biology *85*, 213-218.

Yamamoto, T., Taya, S., and Kaibuchi, K. (1999). Ras-induced transformation and signaling pathway. Journal of biochemistry *126*, 799-803.

Yeatman, T.J. (2004). A renaissance for SRC. Nature reviews. Cancer *4*, 470-480.

Yoshimura, Y., and Miki, H. (2011). Dynamic regulation of GEF-H1 localization at microtubules by Par1b/MARK2. Biochemical and biophysical research communications *408*, 322-328.

Zahradka, P., Storie, B., and Wright, B. (2009). IGF-1 receptor transactivation mediates Src-dependent cortactin phosphorylation in response to angiotensin II. Canadian journal of physiology and pharmacology *87*, 805-812.

Zhang, D., Wang, Z., Jin, N., Li, L., Rhoades, R.A., Yancey, K.W., and Swartz, D.R. (2001). Microtubule disruption modulates the Rho-kinase pathway in vascular smooth muscle. Journal of muscle research and cell motility *22*, 193-200.